X chromosome-dependent disruption of placental regulatory networks in hybrid dwarf hamsters

Thomas D. Brekke[1,2,$], Emily C. Moore[1,$], Shane C. Campbell-Staton[1,3], Colin M. Callahan[1], Zachary A. Cheviron[1], and Jeffrey M. Good[1,*]

Disruption of placental gene expression contributes to several congenital developmental disorders in humans, and may play an important role in the evolution of reproductive barriers between species. The placenta is also highly enriched for interacting genes showing parent-of-origin or imprinted expression, which is thought to have evolved to mitigate parental conflict within this extra-embryonic tissue. However, relatively little is known about the broader organization, functional integration, and evolution of placental gene expression networks across species. Here we used a systems genetics approach to examine the genetic and regulatory underpinnings of placental overgrowth in hybrids between two species of dwarf hamsters (*Phodopus sungorus* and *P. campbelli*). Using quantitative genetic mapping and mitochondrial substitution lines, we show that the X chromosome is the major maternal factor explaining massive parent-of-origin dependent placental overgrowth in hybrids. Mitochondrial interactions did not contribute to abnormal hybrid placental development, and there was only weak correspondence between placental disruption and early embryonic growth phenotypes. In parallel, genome-wide analyses of placental transcriptomes from the parental species and first and second-generation hybrids revealed a central group of co-expressed X-linked and autosomal genes that were highly enriched for maternally-biased expression. Expression of this core placental regulatory network was strongly correlated with placental growth and showed widespread misexpression dependent on epistatic interactions with X-linked hybrid incompatibilities. Silencing of the paternal X chromosome and most candidate paternally imprinted autosomal genes appeared unperturbed in the same genetic crosses. Collectively, our results indicate that the X chromosome plays a prominent role in the evolution of placental gene expression and the rapid accumulation of hybrid developmental barriers between mammalian species.

Introduction

Developing mammalian embryos depend on the extra-embryonic placenta for a broad array of functions including hormone production, immunity, and as a conduit for maternal nutrients and gas exchange [1,2]. Normal intrauterine development in humans and mice depends on the tightly controlled placental expression of a diverse set of genes [2-4]. Placental gene expression has also likely played an important role in the evolution of mammalian development [5-7]. Indeed, much of the phenotypic diversity across mammalian species is thought to have evolved by changes in gene expression during critical stages of development [8-10]. However, relatively little is known about the broader genomic organization, functional integration, and evolution of placental gene expression networks across species [11].

The placenta is characterized by two unusual regulatory phenomena that likely play critical roles in its evolution. First, the placenta is highly enriched for genes showing monoallelic expression due to epigenetic silencing of one parental allele (i.e., genomic imprinting, [12-14]). Genomic imprinting is thought to have evolved to help resolve fitness conflicts between maternally and paternally-inherited alleles (i.e., kinship or parental conflict theory [15]). While perhaps only ~100-200 autosomal genes show strongly imprinted expression across tissues [14], disruption of genomic imprinting has emerged as an important cause of congenital disorders in humans [16,17] and as a potential driver of reproductive barriers between species [18,19]. Second, many mammals achieve dosage compensation in extra-embryonic tissues through imprinted paternal X chromosome inactivation (i.e., imprinted XCI [12, 20-22]), representing a striking deviation from random XCI found in most somatic cells of placental mammals [23,24]. The X chromosome in general, and imprinted XCI in particular, has been shown to play important roles in placental development [25,26]. Moreover, the mouse X chromosome appears enriched for genes preferentially expressed in the placenta [27].

$ TDB and ECM contributed equally to this work
[1] Division of Biological Sciences, University of Montana, Missoula, MT, USA
[2] School of Natural Sciences, Bangor University, Bangor, LL57 2UW, United Kingdom
[3] Department of Ecology and Evolutionary Biology; Institute for Society and Genetics, University of California, Los Angeles, CA
* To whom correspondence should be addressed, t.brekke@bangor.ac.uk (TDB), emily.christine.moore@gmail.com (ECM), jeffrey.good@umontana.edu (JMG)

Resolution of genetic conflict may explain the origin of genomic imprinting in mammals [15]; however, theory also predicts that once imprinting is established adaptation among interacting genes can drive the evolutionary expansion of regulatory networks of similarly imprinted genes [19, 25, 28-30]. Given the relative scarcity of autosomal imprinting overall [14], the X chromosome is expected to harbor the majority of genes showing imprinted (maternal) placental expression in species with imprinted XCI. Thus, co-evolutionary interactions between the maternal X chromosome and maternally expressed autosomal genes should be relatively common within placental regulatory pathways. Despite these predictions, the overall importance of the X chromosome to the evolution of placental gene expression remains unclear. Many molecular genetic studies on the placenta have focued on established disease models or targeted genetic manipulations of imprinted autosomal genes (e.g., gene knockdowns or knockouts [31]), revealing fundamental insights into the mechanisms and functional consequences of genomic imprinting in the placenta and other tissues. In parallel, meta-analyses of expression data have revealed that clusters of imprinted autosomal genes appear to fall within larger networks of co-expressed genes that include both imprinted and bi-allelically expressed loci [11, 32]. The extent and functional relevance of such regulatory networks remain unclear, but the emerging model of genome-wide networks of imprinted and non-imprinted genes represents a conceptual shift from the view of imprinting controlled primarily through local cis-regulatory effects [29].

Parent-of-origin effects for abnormal embryonic and placental growth are common in mammalian hybrids [33, 34], suggesting that hybrid systems may provide powerful models for understanding how the evolution of gene expression impacts placental development. Here, we focus on crosses between two closely related species of dwarf hamsters (*Phodopus sungorus* and *P. campbelli*) that yield strong parent-of-origin growth effects in reciprocal F_1 crosses [34]. Extensive placental overgrowth and disrupted embryonic development occur in hybrid crosses when the mother is *P. sungorus* (female *P. sungorus* x male *P. campbelli*; hereafter S×C), often resulting in hybrid and maternal death during birth. The reciprocal cross (female *P. campbelli* x male *P. sungorus*; hereafter c×s) results in normal embryonic development, although adult hybrid males are smaller [34] and completely sterile [35, 36]. Intrinsic postzygotic reproductive isolation (i.e., hybrid inviability or sterility) generally tends to be asymmetric in reciprocal crosses between closely-related species due to incompatible interactions at sex-linked or imprinted loci [37]. Although the genetic architecture of hybrid placental dysplasia has not been determined in dwarf hamsters, massively overgrown F_1 hybrid S×C placenta do show extensive disruption of gene expression pathways that are highly enriched for embryonic growth and genomic imprinting [38]. Building on these previous works, we combine quantitative genetic and transcriptomic analyses to test the hypothesis that the X chromosome plays a central role in the evolution of placental gene expression, embryonic development, and reproductive barriers between species.

Results and Discussion

The quantitative genetic basis of extreme parent-of-origin hybrid overgrowth. We performed two experiments to dissect the genetic basis of asymmetric hybrid placental and embryonic overgrowth. First, mitochondrial incompatibilities are a possible cause of hybrid parent-of-origin dependent growth because of their strict maternal inheritance and fundamental role in cellular respiration [37]. To test this, we introgressed the *P. campbelli* mitochondrial genome into *P. sungorus* over ten backcross generations. We then crossed females of this conplastic line (*P. sungorus*^{mtC}) to *P. campbelli* males, thereby mimicking the overgrown S×C hybrid across the nuclear genome while substituting the *P. sungorus* mitochondria for *P. campbelli* mitochondria (S^{mtC}×C). If hybrid placental overgrowth is caused by deleterious interactions with the maternal *P. sungorus* mitochondrial genome then this cross should recover normal development. Alternatively, if heterospecific mitochondria have no effect on hybrid growth, then S^{mtC}×C hybrids should be similar in size to the overgrown S×C hybrids. In support of the second hypothesis, S^{mtC}×C placentas were found to be extremely large and not statistically different from S×C hybrids (Figure S1; $F_{4,213}$ = 106, P<0.001, ANOVA, Tukey test reveals that S×C and S^{mtC}×C are similar to each other but different from all other cross types).

Next we crossed fertile F_1 hybrid females (c×s) to *P. campbelli* males to generate a backcross (BC) panel of 189 late-term embryos (38 litters, Theiler's Stages 24-27 [39]). In the context of genetic elements with sex-limited inheritance or expression, these backcross hybrids have the same paternal contribution found in overgrown S×C F_1 hybrids, while varying the species origin of maternally inherited alleles. Using 1,215 single-nucleotide variants (SNVs) derived from double digest restriction-associated DNA (ddRAD) libraries [40], we first constructed a 1,231.7 cM genetic map comprised of 14 major linkage groups (Figure S2 and Table S1). The karyotype of *P. sungorus* is comprised of 14 chromosomes (2N=28, [41], suggesting that each of our major linkage groups correspond to an individual chromosome. The X chromosome was inferred to have the shortest overall genetic distance (35.5 cM or 2.9% of the genetic map), while it appears medium-sized in ranked karyotype analyses (i.e., middle 30%; [41, 42] and comprises ~10% of the haploid female karyotype [43]. The *Phodopus* X chromosome is metacentric with an Xp arm that has been described as heterochromatic [42] and non-recombinant in females of both species and in c×s F_1 hybrids [36]. Our inferred genetic map was consistent with strong repression of recombination on one end of the X chromosome in c×s females, albeit not complete repression as suggested in recent study that quantified signals of mismatch repair through immunolocalization of MLH1 [36].

Using this genetic map, we then tested for quantitative trait loci (QTL) associated with variation in embryo and placenta weights (Figure 1A,B). We observed a single QTL of large effect for placental weight on the X chromosome, with 52.3% of the observed variation in backcross placental weight determined by the genotype of the maternally inherited X chromosome (Figure 1C). We estimated a QTL peak at 31.1cM with a 95% Bayesian confidence interval between 29.6cM and 32.6cM. This QTL localized near the proximal boundary of where we also observed repressed recombination (Figure S3), although the entire X chromosome exceeded a permutation-based significance threshold (P = 0.01). Male and female embryos inheriting a maternal *P. sungorus* X chromosome genotype at this QTL showed an ~60% increase in average placenta weight (Figure 1C inset, $F_{1,179}$ = 178.4, P < 0.0001, ANOVA). No additional placental QTL were uncovered when using sex, developmental stage, and litter size as covariates, nor when using the X-linked QTL as a cofactor.

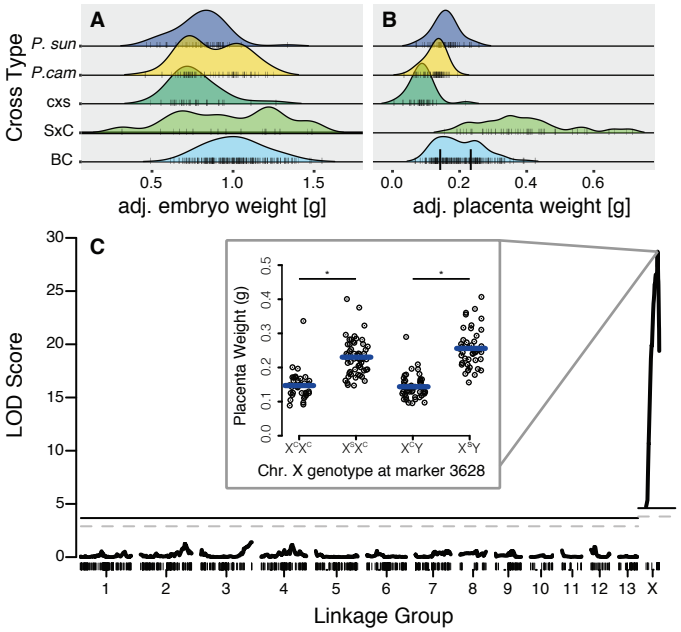

Figure 1. Phenotype Distributions and QTL for placental size. Late term embryo size adjusted for Theiler stage and edema (A) and placenta size adjusted for Theiler stage (B) for *P. sungorus*, *P. campbelli*, reciprocal F_1s, and 189 BC conceptuses. Genetic mapping experiment reveals a single QTL for placenta weight is found on the X chromosome (C). The *P. sungorus* X chromosome increases placenta weight by ~60% (inset, $F_{1,179}$ = 178.4, P << 0.0001, stars indicate significant differences assigned by a Tukey test). Placenta weights are grouped by the genotype at marker 3628. Genotypes are denoted with the maternal allele first followed by the paternal allele. Significance thresholds are denoted by solid (P = 0.01) and dashed (P = 0.05) horizontal lines.

No QTL for embryo weight were recovered in our experiment (P = 0.05 permutation-based significance threshold; Figure S4), despite considerable variation in backcross embryo weights (Figure 1A) and significant overgrowth of S×C embryos when compared to normally developing cross-types [34]. Severe embryonic swelling or edema is common in SxC hybrids [34] and appears to drive overall differences in embryo weights between overgrown SxC hybrids and either species or cxs hybrids (stepwise best model: embryo weight ~ developmental stage + edema; adjusted r2 = 0.40, $F_{2,182}$ = 61.6, P << 0.0001; adjusted embryo weight ~ cross type $F_{3,182}$ = 0.74, P = 0.5312, ANOVA; Figure S5). However, backcross placenta and embryo weights were moderately correlated after adjusting for developmental stage and edema (Figure S6A; adjusted r2 = 0.159, $F_{1,184}$ = 36.0, P << 0.0001, ANOVA), with males showing a stronger correlation than females (males: adjusted r2 = 0.257, $F_{1,95}$ = 33.8, P << 0.0001; females: adjusted r2 = 0.065, $F_{1,88}$ = 7.15, P = 0.0090, ANOVA). When we expanded our analysis of embryonic weights among genotypes to include the backcross, we also detected a small but significant increase in embryo weight in the overgrown crosses after controlling for age and edema (Figure S6B, adjusted r2 = 0.176, $F_{4,376}$ = 21.1, P << 0.0001, ANOVA). These apparent differences in embryonic growth were likely too subtle to detect in our QTL mapping experiment.

A positive parent-of-origin correlation between hybrid placental and embryonic growth effects has been observed in some mammal hybrids (e.g., [44, 45]), providing a possible mechanistic link between the disruption of early development and extreme adult parent-of-origin growth effects observed in many mammal hybrids [34]. Our quantitative results underscore that the relationship between placental and embryonic growth may be weak early in development, especially given the difficulty of differentiating the effects of edema and other developmental defects from overall embryonic growth (Figures S5, S6). Consistent with this, parent-of-origin placental growth effects previously described in some mouse [46, 47] and equine hybrids [48] also were not strongly correlated with hybrid embryonic growth. Regardless of the functional relationship between gross placental and embryonic growth phenotypes, our results show that the species origin of the maternal X chromosome is the major genetic factor responsible for placental overgrowth in hamster hybrids. Reproductive barriers between species often evolve through negative epistatic interactions between two or more loci, generally referred to Dobzhansky-Muller incompatibilities (DMIs) ([49-51], see also [52]). DMIs disproportionately involve X-linked loci, a phenomenon known as the large X-effect [53]. Hybrid incompatibilities presumably occur between the maternally inherited *P. sungorus* X chromosome and *P. campbelli* autosomal loci (e.g., dominant, recessive, or imprinted incompatibilities). However, paternal loci were invariant in our backcross and thus paternal contributions to putative X-autosome mismatches were not directly mappable in this experiment.

Large-X effects for placental dysplasia are perhaps not surprising given the central role that the X chromosome tends to play in the evolution of reproductive isolation [37, 53-55] and the parent-of-origin dependent nature of placental hybrid inviability in dwarf hamsters [34] (Figure1). However, placental overgrowth is also strongly associated with widespread disruption of autosomal regulatory pathways [38] that could manifest entirely from hybrid incompatible interactions between imprinted autosomal

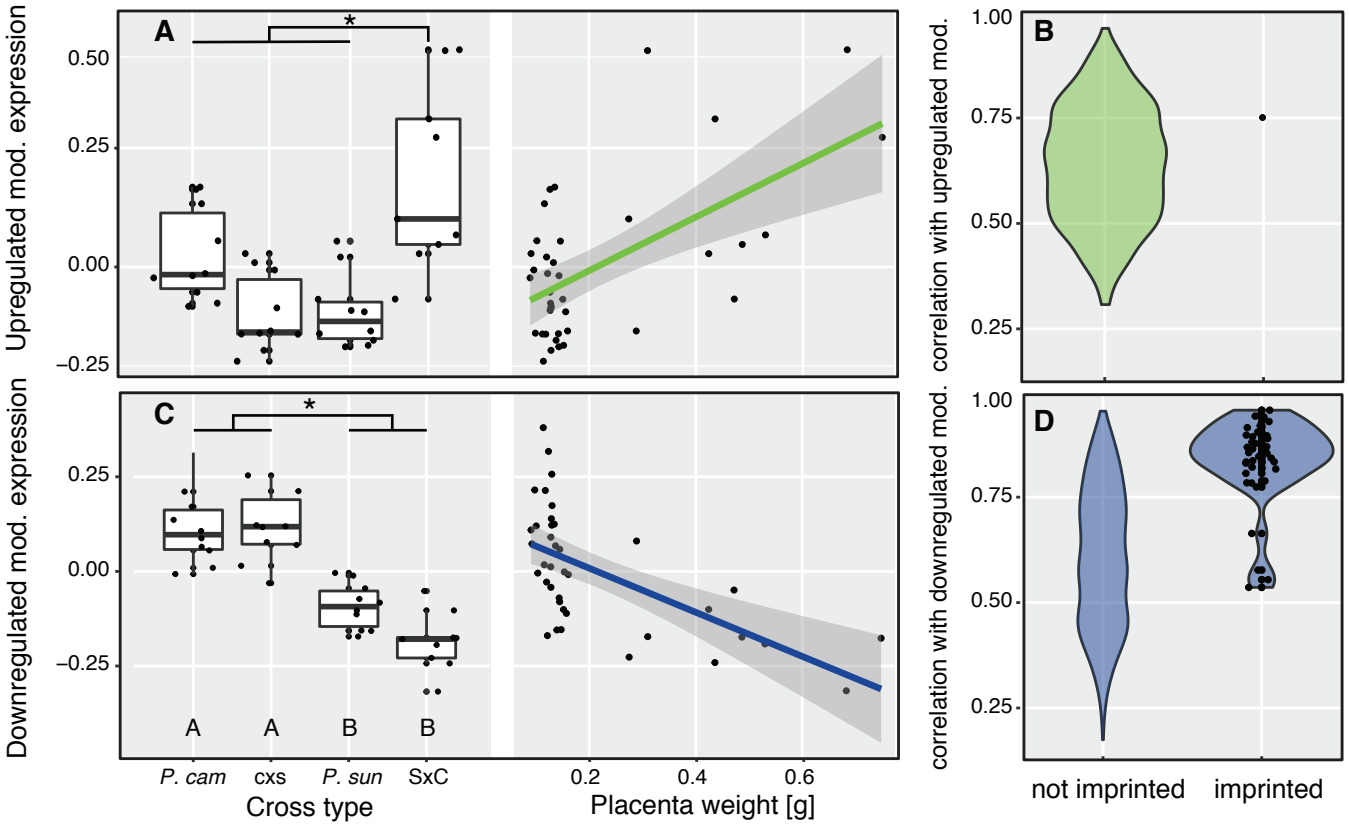

Figure 2. F1 placenta size-associated gene expression modules. Eigengene gene expression values summarize the group of genes that are upregulated (A, B) and downregulated (C,D) in overgrown SxC placentas, shown as differing by cross type (transgressive expression) and placental size (association with hybrid incompatibility phenotype). The downregulated F1 module is enriched for highly connected genes from the candidate set of imprinted genes showing maternal bias in [38] (D). Data points rendered only for imprinted genes in B and D.

genes. Our mapping results rule out this possibility. Strikingly, large effect X-linked QTL also underlie placental dysplasia in hybrid deer mice [44] and house mice [46, 56]. In all three rodent systems, the imprinted XCI occurs in the placenta and incompatibilities on the maternally inherited X chromosome emerge as a central genetic determinant of placental overgrowth in hybrids.

Networks of placental gene expression. We previously demonstrated extensive parent-of-origin dependent disruption of hybrid gene expression [38], with hundreds of genes significantly up- or down-regulated in overgrown S×C hybrid placenta relative to both species (i.e., transgressive expression) [38]. Examination of allele-specific expression revealed 88 candidate imprinted genes in the placenta overall, with 79 genes showing strong bias towards maternal expression (i.e., paternally imprinted). Notably, 68% of candidate imprinted genes (60 genes) showed transgressive expression in overgrown hybrids, suggesting an important link between misexpression of autosomal genes with biased parent-of-origin expression and placental overgrowth. Imprinted XCI was not disrupted in F_1 hybrids. In contrast to a predominantly autosomal regulatory phenotype in F_1 hybrid placenta, our backcross experiments indicated that S×C F_1 hybrid placental overgrowth was likely caused by genetic incompatibilities exposed on the maternally inherited *P. sungorus* X chromosome (Figure 1C).

Motivated by these parallel observations, we sought to identify groups of co-expressed genes associated with overgrowth phenotypes exposed in both of our hybrid F_1 and backcross models of placental dysplasia. We first used our published late-term placental expression data to construct weighted gene co-expression networks using WGCNA [57] (n=39 placental transcriptomes, 5 males and 5 females per cross-type, one female SxC sample was removed during filtering, Figure S7). This network approach uses adjacency correlation matrices to identify hierarchical clusters of co-expressed genes [58], enabling the reduction of complex clusters into representative expression profiles (i.e., module eigengenes) defined as the first component of a principle component analysis.

Network-based re-analysis of filtered transcriptomes from both species and the reciprocal hybrids placed 11,392 genes into 29 signed clusters, or 'modules,' of non-overlapping gene sets. This gene set included 70 candidate imprinted genes [38], after filtering. For each module, expression values were summarized with an 'eigengene', or the principal component capturing the largest proportion of the variance in gene expression. We then assessed each module for mode of eigengene inheritance and association with placental phenotypes (Table S2; Figure S8). Two key gene networks emerged from this F_1 analysis. One module was comprised of 565 genes that tended to be highly expressed in S×C hybrid placenta relative to all other genotypes. The eigengene summary for this module was

positively correlated with placental weights (Figure 2A), and included only one candidate imprinted gene (Figure 2B). The other module was comprised of 1160 genes that tended to show lower summary expression in S×C hybrid placenta (Figure 2C). Expression of this downregulated set was negatively correlated with placental weights (Figure 2C), and included nearly half (44%) of the downregulated transgressive genes identified previously [38]. Eigengene expression for this module exhibited a stronger parent-of-origin mode of inheritance than the upregulated set (Figure 2C), and was positively correlated with candidate imprinted gene expression (Figure 2D). These findings mirror results from pairwise contrasts where overgrown S×C placentas showed an overall reduction in the expression levels of several putatively imprinted genes (Figure 3) [38]. Indeed, the downregulated module included ~50% of the candidate placental imprinted genes overall (36 of 70 genes, Table S2, P << =0.0001).

To test for links between our backcross QTL mapping experiment and emergent patterns of placental expression in F_1 hybrid models, we generated an additional 24 transcriptomes from backcross placentas (12 large placentas including six males and six females; 12 normal sized placentas including six males and six females; 11,396 genes placed in the network). One large placenta female was removed from the analysis during outlier filtering (Figure S9). The recombinant genotypes within this backcross sample allow us to more clearly differentiate disrupted expression in overgrown hybrid placenta versus species differences (*P. sungorus* versus *P. campbelli*) or interspecific hybridization per se (hybrids versus parental species).

WGCNA analysis of the backcross transcriptomes revealed seven modules that were correlated with placenta weights. No clusters were significantly associated with embryo weights after controlling for developmental stage and sex (Table S3). Only about one-third of the core genes included in the upregulated and downregulated F_1 modules were captured in the seven placenta-associated backcross modules (563 of 1725 genes). However, most of these overlapping genes (>90%, 513 of 563) were derived from the downregulated F_1 S×C module (Table S3). Further, the backcross module that was most strongly associated with placental weights (432 genes) tended to show lower summary expression in overgrown backcross placenta (Figure 4A). This downregulated backcross module was also highly enriched for autosomal imprinting (33 candidate imprinted genes, P << 0.0001), X-linkage (25 genes, P < 0.01), and for genes in the downregulated F_1 S×C module (206 gene, P << 0.0001; Table S3; Figures 4, S10). In concordance with the overlap between gene lists, genes that were positively correlated with F_1 downregulated module eigengene were also positively correlated with the BC downregulated module eigengene (Figure S11), indicating module conservation.

Connectivity within scale-free expression networks is commonly defined by the extent to which the expression

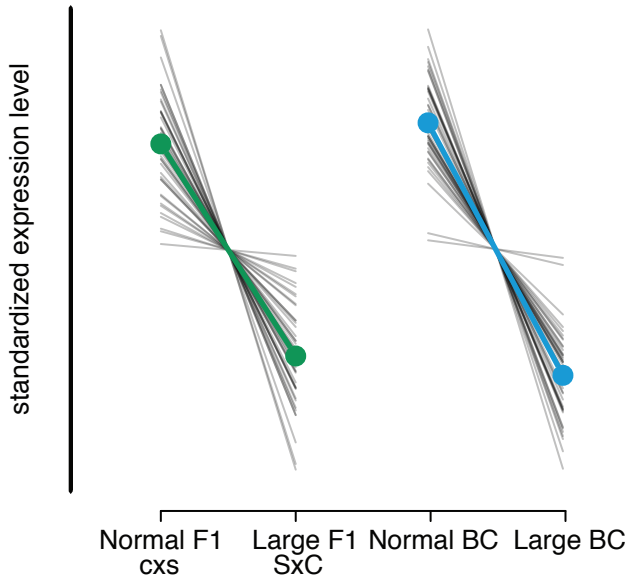

Figure 3. Reduction in candidate imprinted gene expression in overgrown F_1 and BC placentas. Each gray line represents the change in relative expression of a candidate imprinted gene in normal (non-dysplastic) and large (dysplastic) hybrid placentas. Both F_1 and BC experiments demonstrate reduced gene expression of genes showing parent-of-origin bias accompanying placental overgrowth (grand mean indicated by thicker line).

level of a given gene is correlated with the expression of other genes. We found that candidate imprinted genes were much more highly connected than non-imprinted genes within the downregulated, placenta-associated backcross module (Figure 4B). Co-expression modules are usually characterized by a few highly connected “hub” genes [59, 60]. We found that the top 5% most connected (hub) genes in the downregulated module were involved in 60% (300) of the top 500 pairwise interactions (Figure 4C, hub interactions indicated by thicker lines and larger circles). Candidate imprinted genes were overrepresented as hub genes in this network — one third of hub genes (8 of 21, enrichment binomial exact test P << 0.0001) were candidate imprinted loci with maternally-biased expression, including the top five most highly connected genes (*Plxdc2, Procr, Scara5, CD68*, and *Wnt4*). Indeed, nearly half (238) of the top 500 pairwise correlations (blue lines) involved at least one candidate imprinted gene (enrichment binomial exact test P << 0.0001).

These highly-connected, downregulated genes represented many core biological functions of the placenta, ranging from broadly expressed genes involved in growth and development to those with specialized placental function (Table 1). In both rodents and humans, fetal-derived trophoblast cells shape the vasculature at the maternal-fetal interface, allowing for nutrient transport and immune modulation [61]. Notably, in the BC downregulated network, nine of the most connected genes had functions related to coagulation and/or angiogenesis. Endothelial protein C receptor (*ProcR)* is an important anti-coagulant receptor in the trophoblast coagulation cascade [62]. Allelic variants that result in under-expression of *ProcR* are associated with fetal loss in humans [63], and there is some evidence

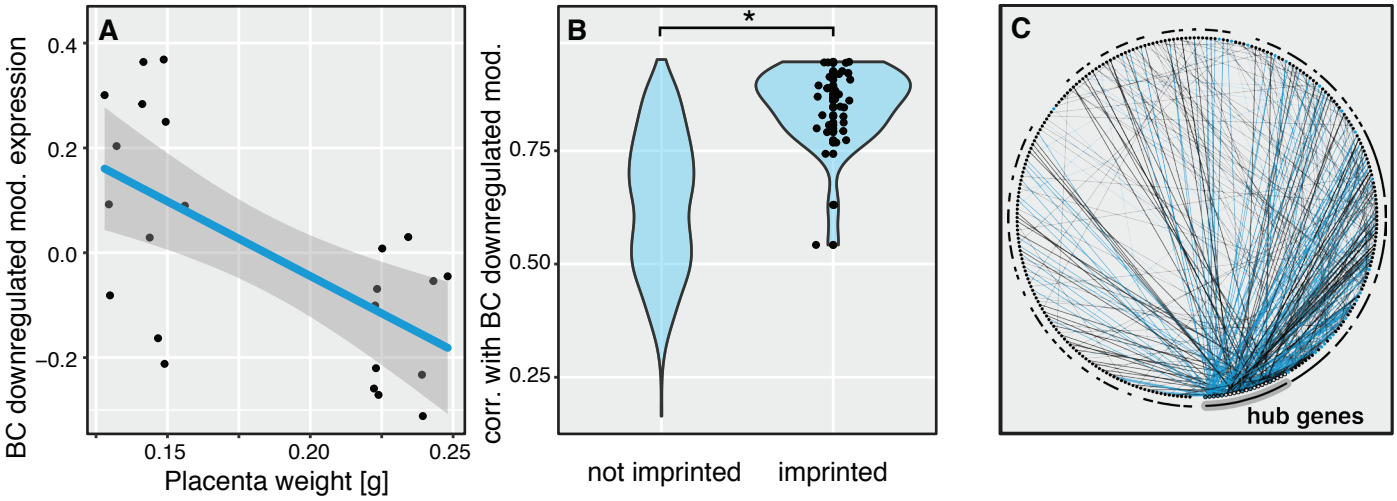

Figure 4. BC downregulated module is associated with placenta size and candidate imprinted genes. (A) Summary expression of the BC downregulated module is significantly associated with placenta size controlling for Theiler stage and sex ($p < 0.001$). (B) This module is enriched for highly connected, candidate imprinted genes ($\mu_{imprinted}$=0.8489±0.015; $\mu_{not\ imprinted}$=0.6370±0.008; Welch's two-sided T-test, $t_{49.315}$=12.255, P<0.0001). Data points rendered only for imprinted genes. (C) The top 500 pairwise connections within this network largely involve the top 5% most connected genes, with interactions involving hub genes have a thicker connecting line and a solid black circumference notation at the interaction partner. Interactions involving a candidate imprinted gene are indicated in blue.

that maternal and fetal *ProcR* genotypes can interact to either prevent or induce placenta-mediated adverse pregnancy outcomes [64]. In a healthy rodent placenta, the coagulation initiating tissue factor is counterbalanced by anti-coagulation proteins produced in differentiated syncytiotrophoblast tissue [64]. Without the early expression of the coagulation cascade in the placenta, development fails [65]; however, low levels of anticoagulants later in development are associated with preeclampsia and pregnancy loss [66]. Several of the hub genes are known to contribute to differentiation of these critical placental layers. For example, *Wnt* signaling is broadly important in placentation and embryonic development, and *Wnt4* specifically may be involved in signaling between the fetal and maternal placental layers [67, 68]. Another such specialized hub gene, *Erv3*, is part of a family of genes co-opted from endogenous retroviruses and are involved in immunomodulation, fusion and differentiation of trophoblasts [69] and are increasingly recognized for their role in regulating placental gene expression [70, 71]. Similarly, the Plexin domain containing 2 (*Plxdc2*) gene encodes an endothelial cell-surface transmembrane receptor [72] that is often co-expressed with *Wnt* signaling genes [73]. Other candidate hub genes play roles in cell-cell adhesion and differentiation [74-76], immune function [77-80], nutrient metabolism and delivery [81-83], and transcriptional regulation [84] (see Table 1).

Overall, our expression data suggest a strong connection between hybrid placental overgrowth, the maternally expressed X chromosome, and the imprinted expression of autosomal genes. Our candidate imprinted gene set included several genes known to be maternally (e.g., *Igf2, Mest, Peg3*) or paternally imprinted (e.g., *Axl, H19, Tfpi2, Wt1*) in mice, as well as several novel candidates including most of the hub genes (Table 1). Confirmation that these candidates reflect the evolution of novel parent-of-origin epigenetic silencing in *Phodopus* (e.g., through DNA methylation or other mechanisms) awaits detailed functional validation beyond the scope of the current study. Others have argued that contamination of maternal blood or tissue may often bias patterns of allele-specific expression in the post-embryonic placenta ([85], but see [86]). We previously found no evidence for systematic maternal contamination of dissected placental tissue in *Phodopus* (i.e., paternal:maternal allele ratios were ~1:1 genome-wide), but it is possible that maternally-biased expression of some of these candidates reflects a large maternal contribution to overall placental expression levels. Indeed, hub genes such as *Wnt4* are thought to be directly involved in signaling between the fetal and maternal placental layers [67, 68]. Regardless of the underlying regulatory mechanisms – epigenomic imprinting or fetal-maternal transcript sharing – our results suggest that X-linked and autosomal genes with maternally-biased expression play a central role in the evolution of placental development and the disruption of placental pathways in hybrids.

The existence of placental networks of maternally-biased gene expression is consistent with some predictions of the co-adaptation theory of gene expression, whereby maternal (or paternal) expression at one gene can select for maternally-biased (or paternally-biased) expression at other positively interacting genes [19, 28, 30, 87]. Such a co-evolutionary process should result in the broader integration of imprinted gene networks and the evolution of separate co-expressed networks of maternally and paternally expressed genes [19, 29]. Furthermore, we propose that the X chromosome, in particular, should play a central role in the evolution of maternally-biased placental networks in some species. The paternal X chromosome remains silenced in extra-embryonic tissues in rodents and some other placental mammals, resulting in imprinted XCI [17, 24, 88] and predominantly maternal expression of hundreds of X-linked genes in the placenta of males and females [20, 21, 38, 89]. Functionally, imprinted XCI contributes the vast majority of maternally expressed genes in the placenta, which as a consequence should favor the

Gene Name	No. interactions in top 500	Module Correlation	Imprinting status	Function (UniProtKB)	Clotting/ angiogenesis	Immune	Growth and development	References
Plxdc2	32	0.9259	candidate	cell surface signaling	maybe		yes	[72]
Procr	28	0.9451	candidate	cell surface signaling, blood coagulation	yes	yes		[62, 64]
Scara5	23	0.9218	candidate	iron transport, blood coagulation	yes		yes	[82]
Cd68	20	0.9133	candidate	immune function		yes		[80]
Wnt4	20	0.9451	candidate	developmental signaling			yes	[67, 68]
Ppard	19	0.9181		transcription factor; steroid hormone receptor			yes	[81]
Adm	18	0.9515		immune function	yes	yes		[78]
Boc	18	0.9217		cell-cell adhesion, tissue differentiation			yes	[76]
Igsf11	17	0.8696		cell-cell adhesion, cell growth, neurogenesis			yes	[75]
Erv3	17	0.9463	candidate	tissue identity and immunomodulation		yes	yes	[69]
Tbc1d2b	16	0.8934		protein modification and transport			yes	[137]
Olfml3	15	0.8884	candidate	developmental signaling	yes			[138]
Lmcd1	13	0.9115		transcription factor			yes	[84]
Fn3krp	12	0.8801		protein modification/glycation	maybe	maybe	yes	[139]
Numbl	11	0.879		cell-cell adhesion, neurogenesis			yes	[74]
Ipmk	11	0.8049		lipid metabolism			yes	[83]
F13a1	10	0.888	candidate	metal binding, blood coagulation	yes			[140]
Pdpn	10	0.8987		cell-cell adhesion, developmental signaling		yes		[77]
Larp6	10	0.824		collagen biosynthesis, fibrosis			yes	[141]
Gypc	10	0.8474		cell membrane stability, red blood cells	yes			[142]
Fut4	10	0.8666		cell-cell adhesion, immune function	maybe	yes		[79]

Table 1. Hub genes in the downregulated, placenta-associated BC module. The top 5% most connected genes in the downregulated module, with connection defined as the number of times the gene was included in the top 500 strongest pairwise correlations in gene expression between genes in the module. Candidate imprinting status [38] and function of the genes are indicated, with emphasis on placental functions of clotting and angiogenesis, immunity, and development.

evolution of maternal expression at interacting autosomal genes. Although XCI appears to be random in the placenta of humans [90] and some other mammals [91-93], male hemizygosity may still favor the evolution of maternal expression at interacting autosomal genes under some conditions [19]. Additionally, the physiological integration of maternal blood supply and trophoblast-generated fetal vasculature is a particularly compelling biological context that should favor the evolution of coordinated maternal-fetal gene expression networks, regardless of the pattern of XCI. Given our data and these general predictions, the broader relevance of X-autosomal gene expression networks to placental evolution and development warrant further consideration.

Towards the genetic basis and architecture of disrupted placental expression. Our transcriptome analyses revealed a central link between the X chromosome and the disruption of autosomal regulatory pathways in the placenta. To integrate our expression and placental phenotypes more directly, we next tested for QTL that explained expression variation in the overall module eigengene. Despite low power due to small sample size (n=23), the X chromosome was a significant predictor of downregulated BC module expression after permutation (Figure S12A). In principle, this signal could represent a predominant contribution of X-linked genes to the eigengene summary of expression within this parent-of-origin module, or a genome-wide trans-regulatory signal dependent on the species origin of the X chromosome. Only ~6% of genes in downregulated backcross module were X-linked (25 of 432, binomial exact test P = 0.006). These genes were significantly under-represented in the correlation network with only 7 of the top 500 pairwise correlations including an X-linked gene (56 pairs expected; binomial exact test $P << 0.0001$). It is also possible that the strong X-linked signal could be a correlated side effect of overall placental phenotypes on expression levels caused by X-linked hybrid incompatibilities. However, we found no significant QTL for the six other expression modules correlated with placental weight (Figure S12B,C), thus this signal is unlikely to be a consequence of a spurious phenotypic correlation.

These results strongly support the hypothesis that X-linked hybrid incompatibilities interacting with a hybrid autosomal background are the primary determinant of disrupted autosomal expression observed in both F_1 and BC hybrids, but the architecture of underlying X-autosome incompatibilities remain unresolved. The current genome assembly for dwarf hamsters is highly fragmented [94] and has not been arranged into an ordered physical map, limiting our ability to fully integrate our transcriptome and quantitative genetic analyses. To begin to overcome these limitations, we designed an exon capture experiment using hybridization probes to enrich SNVs fixed between *P. campbelli* and *P. sungorus* ascertained from the species-specific placental transcriptomes [38]. We then enriched and sequenced these SNV positions in 94 backcross individuals from the mapping panel. After filtering, we were able to anchor 3,616 placenta-expressed genes onto the *Phodopus* genetic map, including 159 X-linked and 34 autosomal imprinted genes (Table S13). An additional 212 X-linked genes were identified based on patterns of inheritance and orthology with mouse, but were not ordered

on the genetic map (371 X-linked genes total). We placed approximately one-third of the BC downregulated network genes (162 of 432 genes) on to the genetic map, including 17 of the 21 hub genes (Table 1). Genes in this anchored network were distributed across 12 of the 13 autosomes and the X chromosome (Figure S14).

If there was a hybrid interaction between the X chromosome and a specific diploid genotype at an autosomal locus that influenced the expression of that gene, then individuals that inherited a maternal P. sungorus X should show a larger change in gene expression for one of the autosomal genotypes than the other. To test for such interactions, we imputed autosomal genotypes for the 23 BC individuals with transcriptome data and calculated expression interaction (EI) scores for all mapped autosomal genes by comparing the difference in fold change in expression of that gene for the two possible autosomal genotypes (i.e., homozygous for the P. campbelli allele or heterozygous) dependent on the genotype of the maternal X chromosome (P. campbelli or P. sungorus). Mapped genes from the BC downregulated module (n=124) showed higher EI scores on average when compared to genes not placed in any WGCNA module ($\mu_{downregulated}$=0.229±0.008, μ_{null}=0.165±0.006, $F_{1,870}$ = 14.13, P =0.0002, ANOVA).

Next we used a linear model to assess the relationship between gene connectivity and EI score in the downregulated module. Hub genes disproportionately overlap with male sterility loci in hybrid mice [95], suggesting that incompatibilities may be more common among highly connected genes. However, we only found support for a slight increase in EI score for genes that were the most connected to the module (Figure 5A, EI ~ module correlation; adjusted r^2 = 0.0243, $F_{1,122}$ = 4.063, P = 0.046). Interestingly, much of the signal for increased EI scores appeared to be driven by candidate imprinted genes rather than hub gene status (Figure 5B, Figure S15, EI ~ candidate imprinting status; adjusted r^2 = 0.059, $F_{1,122}$ = 8.75, P = 0.0037; EI ~ hub; $F_{1,122}$ = 0.005, P = 0.942), again underscoring the central role of genes with maternally biased expression within the downregulated module.

Finally, we polarized EI scores to evaluate specific X-autosome combinations with the downregulated module for candidate hybrid incompatibilities. Within the BC architecture, hybrid incompatibilities involving autosomal recessive or imprinted genes should manifest when the maternally inherited *P. sungorus* X chromosome was combined with maternally inherited *P. campbelli* autosomal allele (all paternal alleles were *P. campbelli*). Consistent with this prediction, we observed positive polarized EI scores for imprinted genes within the downregulated module demonstrating that these expression interactions were driven largely by mismatches between the maternal autosomal and X chromosome genotypes (P = 0.043, Tukey HSD test; non-hub genes, imprinted vs null module, Figure S16A). Furthermore, we found that maternally mismatched imprinted genes in the downregulated module showed larger fold changes when compared to non-imprinted genes regardless of their status as a hub gene (P = 0.045, hub imprinted vs non-imprinted; P < 0.0001, non-hub imprinted vs non-imprinted, Tukey's HSD test, Figure S16B). Collectively, these patterns suggest that maternally expressed imprinted autosomal genes within the downregulated module are more likely to be involved in hybrid incompatible interactions with the X chromosome. One such maternally-biased hub gene was the highly expressed endogenous retrovirus hub gene *Erv3* discussed previously (Figure 5C). Individuals with an interspecific mismatch between the maternally inherited X chromosome (*P. sungorus*) and maternal allele at *Erv3* (*P. campbelli*) showed nearly a one-fold (0.9x) decrease in expression compared to individuals with matching maternal genotypes. Imprinting of *Erv3* appears to be intact in overgrown F1 hybrids [38] and retains maternally-biased allele-specific

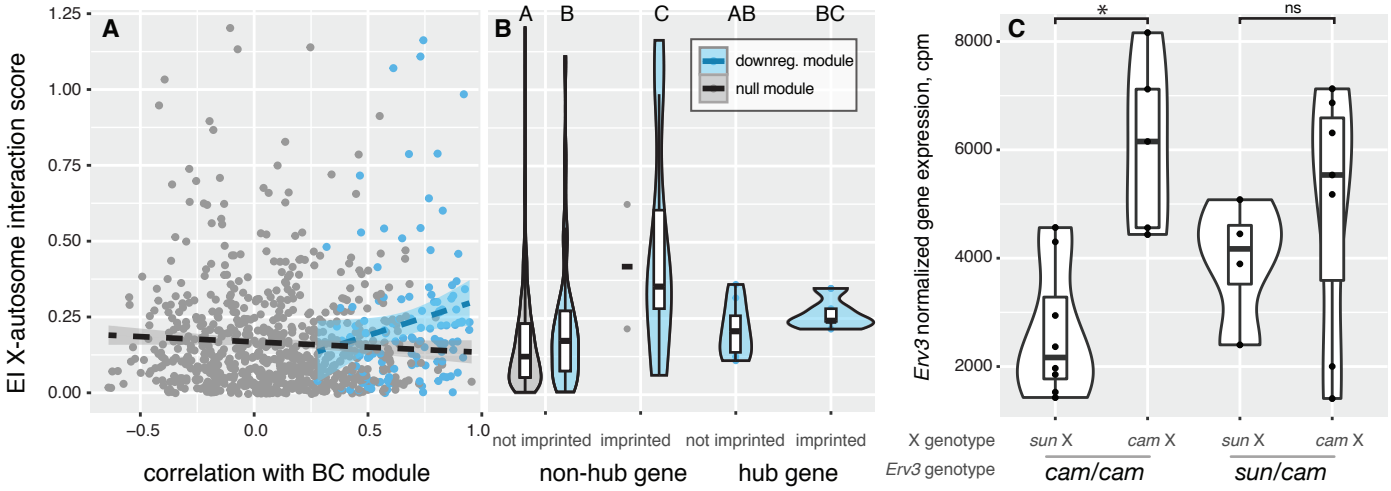

Figure 5. Expression Dobzhansky-Muller incompatibilities exposed in BC hybrids. Greater disruption in the gene expression with X chromosome – autosome mismatch (EI score) is slightly associated with genes more connected in the downregulated BC network module (A). The difference is explained by candidate imprinted genes, rather than highly connected hub genes (B). the EI expression pattern is illustrated with the placental endogenous retrovirus gene *Erv3*, where mismatch between maternal X genotype and maternal *Erv3* genotype results in a greater reduction in gene expression. Letters and star indicate significant differences at p<0.01, assigned by Tukey HSD.

expression in heterozygous BC (Figure S17).

X-linked incompatibilities also underlie parent of origin placental overgrowth in deer mice [44], and house mice [46, 56], but the connection to the broader disruption of placental regulatory pathways has been less clear. Studies in deer mice have linked the X chromosome with disrupted imprinted placental pathways, including the autosomal imprinted gene *Peg3* [96, 97]. X-linked incompatibilities are also the primary cause of hybrid placental overgrowth growth in some hybrid crosses of house mice (*Mus musculus* x *Mus spretus*) [46, 56], but no direct link between disrupted expression of candidate imprinted genes and placental overgrowth [98, 99]. However, a recent genome-wide study on the same *Mus* hybrid system showed transgressive autosomal expression in undergrown hybrid placentas (reciprocal F_1 crosses were not performed), including disruption of the imprinted *Kcnq1* cluster [100]. In these experiments, males show more severe placental phenotypes and disrupted gene expression, which is hypothesized to involve interactions with the imprinted X chromosome [100]. Artificial insemination between more divergent *Mus* species (*Mus musculus* x *Mus caroli*) resulted in massively abnormal placenta showing local demethylation and overexpression of an X-linked retroelement [45]. Similarly, loss of genomic imprinting is correlated with fetal overgrowth produced from assisted reproduction between divergent cattle breeds [101, 102]. Most of these works have focused on F_1 crosses or candidate gene approaches, limiting further insights into the role that X-autosome interactions play in the broader disruption regulatory pathways in hybrid placenta. Building on these previous works, we show that X-linked hybrid incompatibilities underlie the disruption of placental growth, with wide-ranging effects on the misexpression of imprinted autosomal pathways.

Gene expression plays a central role in organismal development and morphological evolution [8-10], but the overall importance of regulatory incompatibilities to species formation has remained unclear [103, 104]. In mammals, considerable progress has been made in linking disruption of specific epigenetic regulatory mechanisms on the X chromosome (e.g., meiotic sex chromosome inactivation) to the evolution of hybrid male sterility during the relatively early stages of speciation [105-107]. However, it has remained unclear if other developmental pathways are also predisposed to disruption in animal hybrids [34, 108]. We suggest that placental development may represent a second developmental hotspot for the evolution of postzygotic reproductive isolation through the widespread disruption of gene expression. Similar to hybrid male sterility [109], the X chromosome also appears to play a central role in the genetic basis of mammalian hybrid inviability caused by placental dysplasia (Figure 1, [44, 46, 56]). Through these parallel systems of hybrid sterility and inviability, a trend is emerging where sex chromosome evolution and genetic conflict within regulatory systems appears to fuel divergence within these key developmental processes [110, 111], ultimately leading to the formation of reproductive barriers between species.

Conclusions

By combining quantitative genetic mapping of placental overgrowth with placental transcriptomic data, we uncovered genome-wide networks of gene expression that were disrupted as a consequence of incompatible genetic interactions with the X chromosome. These data indicate that genetic interactions between the X chromosome and networks of imprinted and non-imprinted genes appear to be critical for proper placental development in hamsters. Qualitatively similar placental [44, 46, 56] and regulatory [96, 97, 100] patterns have been demonstrated in other hybrid rodent systems. As a consequence, we argue that the X chromosome plays a central role in the evolution of placental gene expression networks and the rapid accumulation of hybrid developmental barriers between mammalian species.

Methods

Animals

Experimental animals were drawn from established colonies of wild-derived *P. campbelli* and *P. sungorus* at the University of Montana [34], which were originally established by Kathy Wynne-Edwards [112]. Colonies were maintained as outbred, though overall inbreeding levels are high [113]. All experiments were done in compliance with the University of Montana Institutional Animal Care and Use Committee regulations (animal use protocol 039-13JGDBS-090413).

Experimental crosses

We conducted all advanced genetic crosses through c×s hybrid females as S×C F_1 hybrids generally do not survive birth [34] and c×s males are sterile [35, 36, 114]. To generate conplastic mitochondrial introgression lines, c×s hybrid females were crossed to *P. sungorus* males for ten additional backcross generations. This crossing scheme should recover hamsters that are ~99.9% *P. sungorus* across the nuclear genome but retain the mitochondria of *P. campbelli* (*P. sungorus*^{mtC}). Tenth-generation *P. sungorus*^{mtC} females were crossed to P. campbelli males to test for F_1 overgrowth (S^{mtC}×C). Finally, we performed a backcross experiment by crossing F_1 c×s hybrid females to *P. campbelli* males to generate 189 backcross individuals.

For both experiments, females were sacrificed at late gestation and offspring placentas and embryos were collected, weighed, and snap-frozen on dry ice. Embryos were developmentally scored following [34] to ensure that all offspring were in the final four days of gestation (corresponding to Theiler's Stages 24-27 [39]). Developmental abnormalities such as embryonic fluid accumulation (edema) and embryo loss (reabsorption) were noted, and embryo and placenta weights were assessed

with stepwise model selection and adjusted for variation in edema, litter size and Theiler stage using simple linear models (JMP12).

Genotyping

Genomic DNA was extracted from frozen embryos with a Machery-Nagel Nucleospin Tissue DNA extraction kit (catalog number 740952) following the manufacturer's protocol, except that 5μl RNase-A was added to the column and incubated for 15 minutes at room temperature. Embryo sex was determined using a PCR assay of the Y-linked gene Sry as described in [38].

Double digest restriction-site associated DNA (ddRAD-seq) libraries were generated for 189 backcross individuals (91 females and 98 males) as well as the original colony founders (14 *P. campbelli* individuals and 11 *P. sungorus* individuals) following Peterson and colleagues [115] with the following modifications: we used 1μg of genomic DNA per sample, size selection of adapter-ligated fragments (200-500bp) was done with Agencourt AMPure XP beads, and both the size selection and PCR amplification were done prior to sample pooling to assure more even representation across samples. We digested DNA using the high-fidelity restriction enzyme SbfI-HF (New England BioLabs, catalog number R3642L), followed by MspI (New England BioLabs, catalog number R0106L) both with the CutSmart buffer (New England BioLabs). Libraries were prepared with dual barcoding scheme incorporating both Illumina indexes and in-line barcodes to uniquely identify each sample [115]. Combined sample pools were sequenced on 50% of an Illumina HiSeq 2500 lane in rapid-run mode and then on 50% of a lane of Illumina Hiseq 2500 in normal mode at the University of Oregon Genomics and Cell Characterization Core Facility. All samples were sequenced in both lanes and combined for subsequent analyses.

Multiplexed ddRAD libraries were cleaned and demultiplexed with Stacks (v1.20) process_radtags (parameters -e sbfI --renz_2 mspI -r -c -q) [116]. An initial list of unique RADtags (unique sequences drawn from the pool of sequenced reads) from both read pairs was generated using ustacks (-H -r -d) using data from one female founder from each species. RADtag reference libraries were then generated using cstacks (-n 4). Reads from all the colony founders were aligned to the RADtag reference library with bwa-mem (v0.7.9a) [117] and single-nucleotide variants (SNVs) were called with the GATK HaplotypeCaller (v3.1-1, -stand_call_conf 30) [118,119]. All SNVs that were polymorphic within a species in our colony were filtered out using GATK selectVariants (v3.1-1). Backcross individuals were genotyped at the ascertained SNVs sites using GATK UnifiedGenotyper (v3.1-1, -stand_call_conf 30)[119].

We designed a targeted capture based on the two species-specific placental transcriptomes in order to anchor expressed genes on the genetic map. We designed a custom exon-capture to target 9,756 fixed SNVs between *P. campbelli* and *P. sungorus* ascertained from species-specific transcriptomes (Genbank BioProject JNA306772 and DDBJ/EMBL/GenBank Accessions GEVA00000000 and GEVB00000000, [38]). Exon boundaries were annotated for each transcript with a local BLAT search [120] against the golden hamster (Mesocricetus auratus) reference genome (The Broad Institute Genome Assembly & Analysis Group, MesAur1.0). For each gene, we selected 1-2 SNVs located furthest from inferred exon boundaries and included probes matching both alternative bases to avoid species bias. Capture baits were manufactured by MYcroarray (MyBaits-1 Custom Target Capture Kit).

We selected a subset of 94 individuals (44 males and 50 females) from the backcross panel and prepared Illumina sequencing libraries following the Meyer-Kircher protocol [121]. Ten cycles were used during the indexing PCR step. The indexed libraries were then combined into four pools and target enriched following the MyBaits-1 Custom Target Capture protocol and using mouse CoT-1 DNA supplied by the manufacturer as a blocking agent. The four captured pools were amplified with 20 PCR cycles and quantified with a Kappa qPCR quantification kit (catalog number KK4824) and pooled for sequencing. Enriched libraries were initially sequenced at the University of Montana Genomics Core on an Illumina MiSeq 75bp paired-end sequencing, and followed by one lane of Illumina HiSeq 2500 100bp single-end sequencing at the University of Oregon Genomics and Cell Characterization Core Facility.

Capture sequences were adapter trimmed with Cutadapt (v1.6; -O 5 and -e 0.1 [122] and quality filtered with Trimmomatic (v0.3.2) LEADING:5, SLIDINGWINDOW:4:15, MINLEN:36, and HEADCROP:13 [123]. Filtered reads were then aligned to published transcriptome assemblies [38] and the target SNVs were genotyped with GATK HaplotypeCaller (v3.1-1; -stand_call_conf 30.0 -stand_emit_conf 30) and filtered (selectvariants --restrictAllelesTo BIALLELIC -select "QD > 10.0") so that only high-quality genotypes were used for estimating the location of each gene.

Quantitative genetic analysis

We first constructed a genetic map using RADtag SNVs identified between the strains of *P. campbelli* and *P. sungorus* and the program R/qtl (v1.45; [124]). Putative X-linked RADtags were identified based on segregation patterns in males and females (i.e., markers that were heterozygous or homozygous *P. campbelli* in females and always homozygous *P. campbelli* or *P. sungorus* in males). To build the map, we removed two backcross individuals with low sequencing coverage, identified putative X-linked markers based on Hardy-Weinberg expectations, and dropped all autosomal markers that were genotyped in less than 177 individuals (95%). We formed linkage groups and ordered the markers on each linkage group with the ripple(), compareorder(), and switch.order() functions until each linkage group was a short as possible. Then we sequentially dropped each marker to see if the likelihood of the map improved. Once all poor quality markers were removed, we

repeated the ripple(), compareorder(), and switch.order() functions until the likelihood was maximized. The linkage groups in the final map were ordered by descending length in centiMorgans (cM).

We then used R/qtl [124] to test for quantitative trait loci associated with the variation in embryo and placenta weight in our backcross mapping panel. We first estimated single QTL across the genome for both embryo weight and placenta weight using the extended Haley-Knott method and the imputation method for estimating QTL [125, 126]. Next, we incorporated sex as a covariate and re-estimated the QTL for both phenotypes. For all of single-QTL scans, we used 10,000 permutations to estimate genome-wide significance thresholds for autosomes and 337,364 permutations for the X chromosome. Finally, we used the QTL identified in the first two analyses as additive cofactors and re-scanned for additional QTL that are contingent on the presence of the earlier identified QTL [124]. We used 1,000 permutations for autosome-autosome interactions, 1,687 permutations for autosome-X interactions, and 113,815 permutations for X-X interactions to establish significance thresholds. QTL intervals were established based on 95% Bayesian confidence intervals, and the proportion of phenotypic variance explained by QTL was estimated as 1-10^(-2/n LOD) [115].

To integrate expressed genes on the genetic map, targeted SNV genotypes were used to estimate gene location based on similarity to RADtag genotypes. Following [127], we counted shared genotypes between each RADtag and each gene across all individuals and genes were placed at the location of the RADtag with which they shared the most genotypes. In the event of a tie between multiple RADtags, the gene was placed at the proximal map location (i.e., lower centimorgan) and only genes sharing at least 90% of genotypes with at least one RADtag were placed on the map. Due to the low number of recombinants and the high number of genes, these RADtag-anchored positions represent coarse genetic locations for each gene. Instances where multiple genes were associated with a single RADtag were treated as a single, unordered linkage block. Once integrated, likely genotyping errors in the capture data were identified using calc.errorlod() and the highest errors were extracted with top.errorlod() and a very strict cutoff of 1 such that even moderately questionable genotypes were identified. The genotypes of these sites were removed and then filled in with the fill.geno() function using the imputation method, which imputes the missing genotypes from the surrounding sites for each individual. These corrected genotypes were used for evaluating imprinting status of select genes (see below).

Gene expression analyses

We chose 24 placentas from our backcross mapping panel for genome-wide expression analysis using RNA-seq [128], including six males and six females with large placentas (0.232±0.010g) and six males and six females with normal-sized placentas (mean = 0.140±0.008g) (see Figure 1B). RNA was extracted from whole frozen placenta with an Omega Bio-tek E.Z.N.A. Total RNA Kit I (catalog number R6834) including a DNase digestion following the manufacturer's protocol. All RNA samples were checked for quality and concentration on the bioanalyzer and all samples used had RNA integrity numbers (RIN) greater than 8.0. RNA-seq libraries were constructed from 2 µg of input RNA with the Agilent Sure-Select Strand-Specific RNA-seq Kit (catalog number G9691B) following the manufacturer's recommendations. Libraries were amplified with 14 cycles of PCR, and pooled based on a Kappa qPCR Quantification Kit (catalog number KK4824). The pooled libraries were sequenced with two lanes of Illumina HiSeq2500 100bp single-end sequencing.

RNA-seq data was processed as previously [38]. Briefly, Illumina adapters were trimmed off reads with Cutadapt (v1.6; -O 5 -e 0.1 [122] and quality trimmed with Trimmomatic (v0.3.2; SE -phred 33 LEADING:5 SLIDINGWINDOW:4:15 HEADCROP:13 [123]. While an initial draft of the *P. sungorus* genome has been generated using Illumina shotgun sequencing, current annotation and assembly quality remains insufficient for reference-guided transcriptome analyses [94]. Therefore, reads were aligned with bowtie2 (v2.2.3) [129] to a published de novo placental transcriptome assembly (Genbank BioProject JNA306772 and DDBJ/EMBL/GenBank Accessions GEVA00000000 and GEVB00000000, [38], and filtered for potentially chimeric transcripts using draft genomic resources by excluding 1,422 'genes' with exons that multiply mapped to different contigs. To evaluate expression level, we created a table of counts at the gene level using featureCounts (v1.4.2)[130], which counted fragments (-p) and discarded reads with too long an insert (-P) or are chimeric (-C) or have a mapping quality (-Q) below 20. This table of counts was normalized with the TMM method [131].

Gene networks were analyzed using the WGCNA package (version 1.68 [132]. Briefly, a scale-free topology index was determined by soft thresholding, which was then used to automatically detect signed, Pearson correlated modules via dynamic cutting. We then assessed each module for correlation between the module eigengene and placental and embryonic weight. For those modules with significant correlations after correction for multiple testing, we more stringently tested for associations between traits and modules using an ANOVA model that controlled for developmental stage and sex.

Once module gene composition was finalized, each module was assessed for enrichment of candidate imprinted genes previously identified based on reported patterns of allele-specific expression [38] and genes located on the X chromosome with a binomial exact test (R/stats package 3.6.1). Network connectivity was determined through pairwise correlation between genes, with p-values corrected via qvalue package (version 2.18.) [133]. Hub genes were defined as the top 5% most connected genes in each module. Overlap between F_1 and backcross modules was determined by comparing gene lists to get counts of

shared genes. We also evaluated module conservation by comparing how strongly each gene was correlated to each network across data sets. To connect module conservation to phenotypes, we compared the concordance between each gene and placenta weight across F_1 and backcross datasets using a bivariate correlation (JMP12).

Genotypes at each gene were conservatively generated by evaluating the genotypes at RAD markers flanking each gene placed in the map. If the gene was placed in the same linkage block (exact cM location) as a RADtag, the marker genotype was used for the gene; likewise, if the gene was placed between two markers with the same genotype, the concordant marker genotypes were used for the gene. If the marker genotypes were discordant, the genotype at the gene was left as unknown. To generate the EI score, BC normalized gene expression count tables generated during WGCNA were used to evaluate log2-fold change between X chromosome genotypes by genotype at each autosomal locus, excluding unmapped autosomal genes and genes with imputed genotypes for fewer than 3 individuals each of the four X-by-autosome genotypic classes. We first calculated the absolute value of EI scores, where a value of 0 indicates no difference between the two autosomal genotypes when inheriting different maternal X chromosomes and a value of 1 indicates a one-fold difference in expression between the two autosomal genotypes (i.e., a candidate X-autosome expression interaction). We also considered a polarized version of the statistic where positive values reflect greater change when maternal X and autosomal alleles genotypes were discordant.

$$EI = \left| \log2(\mu\ expression_{X_{cam}Gene_{CC}} - \mu\ expression_{X_{sun}Gene_{CC}}) - \log2(\mu\ expression_{X_{cam}Gene_{SC}} - \mu\ expression_{X_{sun}Gene_{SC}}) \right|$$

Evaluating allelic expression in backcrosses required that we exclude genes in each individual that are homozygous so we restricted our analysis to heterozygous genotypes based on the corrected genotypes. Allelic usage was evaluated similar to [38]: for allele-specific expression in F_1s, we identified maternal and paternal reads for each gene with the modtools package [134, 135], created a table of counts with maternal and paternal columns for each individual, standardized the count table by library size, excluded homozygous sites, and calculated the allelic usage ratio as the average number of paternal alleles divided by total alleles for each gene.

The same procedure in with BC samples resulted in results with considerable noise due to a low number of stringently filtered variants, and thus was complemented by a strategy where reads were aligned to the *P. sungorus* reference transcriptome and genotyped with HaplotypeCaller (GATK 3.8) into a single VCF. We then filtered the VCF to include only variants where the alternate (*P. campbelli*) allele was more common in the BC, and only for candidate imprinted genes previously described [38]. For the remaining 31 candidate imprinted genes with filtered variants, the reference (*P. sungorus*) allele was designated the maternal allele, and the proportion of maternal reads was averaged over all variants. Because there are higher levels of segregating variation in our outbred animals, each variant has somewhat lower confidence about parent of origin; by averaging the signal for allelic usage across all variants we buffered against the risk that any single variant was incorrectly assigned. Using this method, we were able to recover maternal and paternal bias in expression as expected from F_1 data [38]. While the complementary allele-specific expression method described here is subject to mapping bias, it is sufficient in the limited case where the goal is not discovery of novel genes with allelic bias in expression and the more stringent pipeline lacks the power to recover the signal of parent-of-origin expression.

Competing Interests

The authors declare they have no conflict of interest.

Acknowledgements

Ryan Bracewell, Zak Clare-Salzler, Ted Cosart, Kris Crandell, Doug Emlen, Mafalda Ferreira, Lila Fishman, Evgueny Kroll, Lindy Henry, Matt Jones, Sara Keeble, Erica Larson, John McCutcheon, Colin Prather, Brice Sarver, Vanessa Stewart, Dan Vanderpool, Jon Velotta, Paul Vrana, and the UNVEIL network provided helpful comments on data analysis and/or interpretation. Kelly Carrick, Jess Wexler, and the University of Montana LAR staff for helping with animal care. This research was supported by the Eunice Kennedy Shriver National Institute of Child Health and Human Development of the National Institutes of Health (R01-HD073439, R01-HD094787 to JMG), the National Science Foundation (EPSCoR OIA-1736249 to JMG and ZAC; DBI Postdoctoral Fellowship in Biology 1612283 to SCS), a Society for the Study of Evolution Rosemary Grant Award (to TDB), a National Science Foundation Doctoral Dissertation Improvement Grant (DEB-1406754 to TDB), and a David Nicholas Award (to TDB). This study includes research conducted in the University of Montana Genomics Core, supported by a grant from the M.J. Murdock Charitable Trust.

Data availability

Raw sequencing reads are archived at NCBI under BioProject PRJNA306772. Accession numbers for individual libraries are provided in Table S5

References

1. Reik W, Constancia M, Fowden A, Anderson N, Dean W, Ferguson-Smith A, et al. Regulation of supply and demand for maternal nutrients in mammals by imprinted genes. The Journal of Physiology. 2003;547:35-44.

2. Levy O. Innate immunity of the newborn: basic mechanisms and clinical correlates. Nature Reviews Immunology. 2007;7:379-90.

3. Constancia M, Hemberger M, Hughes J, Dean W, Ferguson-Smith A, Fundele R, et al. Placental-specific IGF-II is a major modulator of placental and fetal growth. Nature. 2002;417:945-8.

4. Plasschaert RN, Bartolomei MS. Genomic imprinting in development, growth, behavior and stem cells. Development. 2014;141:1805-13.

5. Haig D. Placental hormones, genomic imprinting, and maternal-fetal communication. Journal of Evolutionary Biology. 1996;9:357-80.

6. Capellini I, Venditti C, Barton RA. Placentation and maternal investment in mammals. The American Naturalist. 2011;177:86-98.

7. Kaneko-Ishino T, Ishino F. Evolution of viviparity in mammals: what genomic imprinting tells us about mammalian placental evolution. Reproduction Fertility and Development. 2019;31:1219-27.

8. King MC, Wilson AC. Evolution at two levels in humans and chimpanzees. Science. 1975;188:107-16.

9. Carroll SB. Evo-devo and an expanding evolutionary synthesis: A genetic theory of morphological evolution. Cell. 2008;134:25-36.

10. Sears KE, Maier JA, Rivas-Astroza M, Poe R, Zhong S, Kosog K, et al. The relationship between gene network structure and expression variation among individuals and species. PLoS Genetics. 2015;11:e1005398.

11. Al Adhami H, Evano B, Le Digarcher A, Gueydan C, Dubois E, Parrinello H, et al. A systems-level approach to parental genomic Imprinting: the imprinted gene network includes extracellular matrix genes and regulates cell cycle exit and differentiation. Genome Research. 2015;25:353-67.

12. Morison IM, Ramsay JP, Spencer HG. A census of mammalian imprinting. Trends in Genetics. 2005;21:457-65.

13. Hudson QJ, Kulinski TM, Huetter SP, Barlow DP. Genomic imprinting mechanisms in embryonic and extraembryonic mouse tissues. Heredity. 2010;105:45-56.

14. Babak T, DeVeale B, Tsang EK, Zhou YQ, Li X, Smith KS, et al. Genetic conflict reflected in tissue-specific maps of genomic imprinting in human and mouse. Nature Genetics. 2015;47:544-9.

15. Haig D. The kinship theory of genomic imprinting. Annual Review of Ecology and Systematics. 2000;31:9-32.

16. Hirasawa R, Feil R. Genomic imprinting and human disease. In: Lipps HJ, Postberg J, Jackson DA, editors. Essays in Biochemistry: Epigenetics, Disease and Behaviour. Essays in Biochemistry. 482010. p. 187-200.

17. Lee JT, Bartolomei MS. X-inactivation, imprinting, and long noncoding RNAs in health and disease. Cell. 2013;152:1308-23.

18. Crespi B, Nosil P. Conflictual speciation: species formation via genomic conflict. Trends in Ecology & Evolution. 2013;28:48-57.

19. Wolf JB, Brandvain Y. Gene interactions in the evolution of genomic imprinting. Heredity. 2014;113:129-37.

20. Xue F, Tian XC, Du FL, Kubota C, Taneja M, Dinnyes A, et al. Aberrant patterns of X chromosome inactivation in bovine clones. Nature Genetics. 2002;31:216-20.

21. Heard E, Disteche CM. Dosage compensation in mammals: fine-tuning the expression of the X chromosome. Genes & Development. 2006;20:1848-67.

22. Al Nadaf S, Deakin JE, Gilbert C, Robinson TJ, Graves JAM, Waters PD. A cross-species comparison of escape from X inactivation in Eutheria: Implications for evolution of X chromosome inactivation. Chromosoma. 2012;121:71-8.

23. Lyon MF. Gene action in X-chromosome of mouse (Mus musculus L). Nature. 1961;190:372-3.

24. Dupont C, Gribnau J. Different flavors of X-chromosome inactivation in mammals. Current Opinion in Cell Biology. 2013;25:314-21.

25. Hemberger M. The role of the X chromosome in mammalian extra embryonic development. Cytogenetic and Genome Research. 2002;99:210-7.

26. McGraw S, Oakes CC, Martel J, Cirio MC, de Zeeuw P, Mak W, et al. Loss of DNMT1o disrupts imprinted X chromosome inactivation and accentuates placental defects in females. PLoS Genetics. 2013;9.

27. Khil PP, Smirnova NA, Romanienko PJ, Camerini-Otero RD. The mouse X chromosome is enriched for sex-biased genes not subject to selection by meiotic sex chromosome inactivation. Nature Genetics. 2004;36:642-6.

28. Wolf JB, Hager R. A maternal–offspring coadaptation theory for the evolution of genomic imprinting. PLoS Biology. 2006;4:2238-43.

29. Patten MM, Cowley M, Oakey RJ, Feil R. Regulatory links between imprinted genes: evolutionary predictions and consequences. Proceedings of the Royal Society B-Biological Sciences. 2016;283:20152760.

30. O'Brien EK, Wolf JB. The coadaptation theory for genomic imprinting. Evolution Letters. 2017;1:49-59.

31. Sanli I, Feil R. Chromatin mechanisms in the developmental control of imprinted gene expression. International Journal of Biochemistry & Cell Biology. 2015;67:139-47.

32. Varrault A, Gueydan C, Delalbre A, Bellmann A, Houssami S, Aknin C, et al. Zac1 regulates an imprinted gene network critically involved in the control of embryonic growth. Developmental Cell. 2006;11:711-22.

33. Vrana PB. Genomic imprinting as a mechanism of reproductive isolation in mammals. Journal of Mammalogy. 2007;88:5-23.

34. Brekke TD, Good JM. Parent-of-origin growth effects and the evolution of hybrid inviability in dwarf hamsters. Evolution. 2014;68:3134-48.

35. Safronova LD, Cherepanova EV, Vasil'eva NY. Specific features of the first meiotic division in hamster hybrids obtained by backcrossing Phodopus sungorus and Phodopus campbelli. Russian Journal of Genetics. 1999;35:184-8.

36. Bikchurina TI, Tishakova KV, Kizilova EA, Romanenko SA, Serdyukova NA, Torgasheva AA, et al. Chromosome synapsis and recombination in male-sterile and female-fertile interspecies hybrids of the dwarf hamsters (Phodopus, Cricetidae). Genes. 2018;9.

37. Turelli M, Moyle LC. Asymmetric postmating isolation: Darwin's corallary to Haldane's rule. Genetics. 2007;176:1059-88.

38. Brekke T, Henry L, Good J. Genomic imprinting, disrupted placental expression, and speciation. Evolution. 2016;70:2690-703.

39. Theiler K. The house mouse: Development and normal stages from fertilization to 4 weeks of age. New York, NY.: Springer-Verlag; 1972. 178 p.

40. Peterson BK, Weber JN, Kay EH, Fisher HS, Hoekstra HE. Double digest RADseq: an inexpensive method for de novo SNP discovery and genotyping in model and non-model species. PLoS One. 2012;7:e37135.

41. Romanenko SA, Volobouev VT, Perelman PL, Lebedev VS, Serdukova NA, Trifonov VA, et al. Karyotype evolution and phylogenetic relationships of hamsters (Cricetidae, Muroidea, Rodentia) inferred from chromosomal painting and banding comparison. Chromosome Research. 2007;15:283-97.

42. Gamperl R, Vistorin G, Rosenkranz W. New observations on karyotype of Djungarian hamster, Phodopus sungorus. Experientia. 1977;33:1020-1.

43. Haaf T, Weis H, Schmid M. A comparative cytogenetic study on the mitotic and meiotic chromosomes in hamster species of the genus Phodopus (Rodentia, Cricetinae). Zeitschrift Fur Saugetierkunde-International Journal of Mammalian Biology. 1987;52:281-90.

44. Vrana PB, Fossella JA, Matteson P, del Rio T, O'Neill MJ, Tilghman SM. Genetic and epigenetic incompatibilities underlie hybrid dysgenesis in Peromyscus. Nature Genetics. 2000;25:120-4.

45. Brown JD, Piccuillo V, O'Neill RJ. Retroelement demethylation associated with abnormal placentation in Mus musculus x Mus caroli hybrids. Biology of Reproduction. 2012;86:88-.

46. Zechner U, Reule M, Orth A, Bonhomme F, Strack B, Guenet JL, et al. An X-chromosome linked locus contributes to abnormal placental development in mouse interspecific hybrids. Nature Genetics. 1996;12:398-403.

47. Kurz H, Zechner U, Orth A, Fundele R. Lack of correlation between placenta and offspring size in mouse interspecific crosses. Anatomy and Embryology. 1999;200:335-43.

48. Allen WR, Skidmore JA, Stewart F, Antczak DF. Effects of fetal genotype and uterine environment on placental development in equids. Journal of Reproduction and Fertility. 1993;98:55-60.

49. Dobzhansky T. Genetics and the Origin of Species. 1st ed. New York: Columbia University Press; 1937. 364 p.

50. Muller HJ. Isolating mechanisms, evolution, and temperature. Biol Symp. 1942;6:71-125.

51. Orr HA, Turelli M. The evolution of postzygotic isolation: accumulating Dobzhansky-Muller incompatibilities. Evolution. 2001;55:1085-94.

52. Bateson W. Heredity and variation in modern lights. In: Seward AC, editor. Darwin and Modern Science. Cambridge: Cambridge University Press; 1909.

53. Coyne JA, Orr HA. Two rules of speciation. In: Otte D, Endler J, editors. Speciation and Its Consequences. Sunderland, MA: Sinauer Associates; 1989. p. 180-207.

54. Turelli M, Orr HA. Dominance, epistasis and the genetics of postzygotic isolation. Genetics. 2000;154:1663-79.

55. Masly JP, Presgraves DC. High-resolution genome-wide dissection of the two rules of speciation in Drosophila. PLoS Biology. 2007;5:1890-8.

56. Hemberger MC, Pearsall RS, Zechner U, Orth A, Otto S, Ruschendorf F, et al. Genetic dissection of X-linked interspecific hybrid placental dysplasia in congenic mouse strains. Genetics. 1999;153:383-90.

57. Langfelder P, Horvath S. WGCNA: an R package for weighted correlation network analysis. Bmc Bioinformatics. 2008;9:559.

58. Zhang B, Horvath S. A general framework for weighted gene co-expression network analysis. Statistical Applications in Genetics and Molecular Biology. 2005;4:17.

59. Ghazalpour A, Doss S, Zhang B, Wang S, Plaisier C, Castellanos R, et al. Integrating genetic and network analysis to characterize genes related to mouse weight. PLoS Genetics. 2006;2:1182-92.

60. Mack KL, Phifer-Rixey M, Harr B, Nachman MW. Gene expression networks across multiple tissues are associated with rates of molecular evolution in wild house mice. Genes. 2019;10.

61. Gris JC, Bouvier S, Cochery-Nouvellon E, Mercier E, Mousty E, Perez-Martin A. The role of haemostasis in placenta-mediated complications. Thrombosis Research. 2019;181:S10-S4.

62. Bouwens EAM, Stavenuiter F, Mosnier LO. Mechanisms of anticoagulant and cytoprotective actions of the protein C pathway. Journal of Thrombosis and Haemostasis. 2013;11:242-53.

63. Cochery-Nouvellon E, Chauleur C, Demattei C, Mercier E, Fabbro-Peray P, Mares P, et al. The A6936G polymorphism of the endothelial protein C receptor gene is associated with the risk of unexplained foetal loss in Mediterranean European couples. Thrombosis and Haemostasis. 2009;102:656-67.

64. Sood R, Kalloway S, Mast AE, Hillard CJ, Weiler H. Fetomaternal cross talk in the placental vascular bed: control of coagulation by trophoblast cells. Blood. 2006;107:3173-80.

65. Isermann B, Sood R, Pawlinski R, Zogg M, Kalloway S, Degen JL, et al. The thrombomodulin-protein C system is essential for the maintenance of pregnancy. Nature medicine. 2003;9:331-7.

66. Ebina Y, Ieko M, Naito S, Kobashi G, Deguchi M, Minakami H, et al. Low levels of plasma protein S, protein C and coagulation factor XII during early pregnancy and adverse pregnancy outcome. Thrombosis and Haemostasis. 2015;114:65-9.

67. Sonderegger S, Pollheimer J, Knoefler M. Wnt Signalling in Implantation, Decidualisation and Placental Differentiation - Review. Placenta. 2010;31:839-47.

68. Knoefler M, Pollheimer J. Human placental trophoblast invasion and differentiation: a particular focus on Wnt signaling. Frontiers in genetics. 2013;4:190.

69. Mangeney M, Renard M, Schlecht-Louf G, Bouallaga I, Heidmann O, Letzelter C, et al. Placental syncytins: Genetic disjunction between the fusogenic and immunosuppressive activity of retroviral envelope proteins. Proceedings of the National Academy of Sciences of the United States of America. 2007;104:20534-9.

70. Pavlicev M, Hiratsuka K, Swaggart KA, Dunn C, Muglia L. Detecting endogenous retrovirus-driven tissue-specific gene transcription. Genome Biology and Evolution. 2015;7:1082-97.

71. Chuong EB. The placenta goes viral: Retroviruses control gene expression in pregnancy. PLoS Biology. 2018;16:e3000028.

72. Cheng G, Zhong M, Kawaguchi R, Kassai M, Al-Ubaidi M, Deng J, et al. Identification of PLXDC1 and PLXDC2 as the transmembrane receptors for the multifunctional factor PEDF. eLife. 2014;3:e05401.

73. Miller SFC, Summerhurst K, Runker AE, Kerjan G, Friedel RH, Chedotal A, et al. Expression of Plxdc2/TEM7R in the developing nervous system of the mouse. Gene Expression Patterns. 2007;7:635-44.

74. Wilson A, Ardiet DL, Saner C, Vilain N, Beermann F, Aguet M, et al. Normal hemopoiesis and lymphopoiesis in the combined absence of numb and numblike. Journal of Immunology. 2007;178:6746-51.

75. Jang S, Oh D, Lee Y, Hosy E, Shin H, van Riesen C, et al. Synaptic adhesion molecule IgSF11 regulates synaptic transmission and plasticity. Nature Neuroscience. 2016;19:84-93.

76. Zakaria M, Ferent J, Hristovska I, Laouarem Y, Zahaf A, Kassoussi A, et al. The Shh receptor Boc is important for myelin formation and repair. Development. 2019;146:dev172502.

77. Astarita JL, Acton SE, Turley SJ. Podoplanin: emerging functions in development the immune system and cancer. Frontiers in Immunology. 2012;3:283.

78. Li M, Schwerbrock NMJ, Lenhart PM, Fritz-Six KL, Kadmiel M, Christine KS, et al. Fetal-derived adrenomedullin mediates the innate immune milieu of the placenta. Journal of Clinical Investigation. 2013;123:2408-20.

79. Wang H, Morales-Levy M, Rose J, Mackey LC, Bodary P, Eitzman D, et al. α(1,3)-Fucosyltransferases FUT4 and FUT7 control murine susceptibility to thrombosis. American Journal of Pathology. 2013;182:2082-93.

80. Chistiakov DA, Killingsworth MC, Myasoedova VA, Orekhov AN, Bobryshev YV. CD68/macrosialin: not just a histochemical marker. Laboratory Investigation. 2017;97:4-13.

81. Schmidt A, Endo N, Rutledge SJ, Vogel R, Shinar D, Rodan GA. Identification of a new member of the steroid-hormone receptor superfamily that is activated by a peroxisome proliferator and fatty-acids. Molecular Endocrinology. 1992;6:1634-41.

82. Li JY, Paragas N, Ned RM, Qiu A, Viltard M, Leete T, et al. Scara5 Is a ferritin receptor mediating non-transferrin iron delivery. Developmental Cell. 2009;16:35-46.

83. Malabanan MM, Blind RD. Inositol polyphosphate multikinase (IPMK) in transcriptional regulation and nuclear inositide metabolism. Biochemical Society Transactions. 2016;44:279-85.

84. Ferreira DMS, Cheng AJ, Agudelo LZ, Cervenka I, Chaillou T, Correia JC, et al. LIM and cysteine-rich domains 1 (LMCD1) regulates skeletal muscle hypertrophy, calcium handling, and force. Skeletal Muscle. 2019;9:26.

85. Wang X, Soloway PD, Clark AG. A survey for novel imprinted genes in the mouse placenta by mRNA-seq. Genetics. 2011;189:109-22.

86. Finn EH, Smith CL, Rodriguez J, Sidow A, Baker JC. Maternal bias and escape from X chromosome imprinting in the midgestation mouse placenta. Developmental Biology. 2014;390:80-92.

87. Wolf JB. Evolution of genomic imprinting as a coordinator of coadapted gene expression. Proceedings of the National Academy of Sciences of the United States of America. 2013;110:5085-90.

88. Takagi N, Sasaki M. Preferential inactivation of paternally derived X-chromosome in extraembryonic membranes of mouse. Nature. 1975;256:640-2.

89. Al Nadaf S, Waters PD, Koina E, Deakin JE, Jordan KS, Graves JAM. Activity map of the tammar X chromosome shows that marsupial X inactivation is incomplete and escape is stochastic. Genome Biology. 2010;11:R122.

90. Moreira de Mello JC, Souza de Araujo ES, Stabellini R, Fraga AM, Santana de Souza JE, Sumita DR, et al. Random X inactivation and extensive mosaicism in human placenta revealed by analysis of allele-specific gene expression along the X chromosome. PLoS One. 2010;5:e10947.

91. Okamoto I, Patrat C, Thepot D, Peynot N, Fauque P, Daniel N, et al. Eutherian mammals use diverse strategies to initiate X-chromosome inactivation during development. Nature. 2011;472:370-4.

92. Wang X, Miller DC, Clark AG, Antczak DF. Random X inactivation in the mule and horse placenta. Genome Research. 2012;22:1855-63.

93. Zou H, Yu D, Du X, Wang J, Chen L, Wang Y, et al. No imprinted XIST expression in pigs: biallelic XIST expression in early embryos and random X inactivation in placentas. Cellular and Molecular Life Sciences. 2019;76:4525-38.

94. Bao R, Onishi KG, Tolla E, Ebling FJP, Lewis JE, Anderson RL, et al. Genome sequencing and transcriptome analyses of the Siberian hamster hypothalamus identify mechanisms for seasonal energy balance. Proceedings of the National Academy of Sciences of the United States of America. 2019;116:13116-21.

95. Morgan K, Harr B, White MA, Payseur BA, Turner LM. Disrupted gene networks in subfertile hybrid house mice. Molecular Biology and Evolution. 37:1547-62.

96. Duselis A, Wiley C, Vrana PB. A maternal effect controls genomic imprinting and placental growth in Peromyscus hybrids. Placenta. 2004;25:A11-A.

97. Loschiavo M, Nguyen QK, Duselis AR, Vrana PB. Mapping and identification of candidate loci responsible for Peromyscus hybrid overgrowth. Mammalian Genome. 2007;18:75-85.

98. Shi W, Lefebvre L, Yu Y, Otto S, Krella A, Orth A, et al. Loss-of-imprinting of Peg1 in mouse interspecies hybrids is correlated with altered growth. genesis. 2004;39:65-72.

99. Zechner U, Shi W, Hemberger M, Himmelbauer H, Otto S, Orth A, et al. Divergent genetic and epigenetic post-zygotic isolation mechanisms in Mus and Peromyscus. Journal of Evolutionary Biology. 2004;17:453-60.

100. Arévalo L, Gardner S, Campbell P. Haldane's rule in the placenta: sex-biased misregulation of the Kcnq1 imprinting cluster in hybrid mice. bioRxiv. 2020;doi: https://doi.org/10.1101/2020.05.07.082248.

101. Chen ZY, Hagen DE, Elsik CG, Ji T, Morris CJ, Moon LE, et al. Characterization of global loss of imprinting in fetal overgrowth syndrome induced by assisted reproduction. Proceedings of the National Academy of Sciences of the United States of America. 2015;112:4618-23.

102. Chen ZY, Hagen DE, Wang JB, Elsik CG, Ji TM, Siqueira LG, et al. Global assessment of imprinted gene expression in the bovine conceptus by next generation sequencing. Epigenetics. 2016;11:501-16.

103. Butlin R, Debelle A, Kerth C, Snook RR, Beukeboom LW, Castillo Cajas RF, et al. What do we need to know about speciation? Trends in Ecology & Evolution. 2012;27:27-39.

104. Guerrero RF, Posto AL, Moyle LC, Hahn MW. Genome-wide patterns of regulatory divergence revealed by introgression lines. Evolution. 2016;70:696-706.

105. Bhattacharyya T, Gregorova S, Mihola O, Anger M, Sebestova J, Denny P, et al. Mechanistic basis of infertility of mouse intersubspecific hybrids. Proceedings of the National Academy of Sciences of the United States of America. 2013;110:E468-E77.

106. Davis BW, Seabury CM, Brashear WA, Li G, Roelke-Parker M, Murphy WJ. Mechanisms underlying mammalian hybrid sterility in two feline interspecies models. Molecular Biology and Evolution. 2015;32:2534-46.

107. Larson E, Vanderpool D, Keeble S, Dean M, Good J. The composite regulatory basis of the large X-effect in mouse speciation. Molecular Biology and Evolution. 2017;34:282-95.

108. Coyne JA, Orr HA. Speciation. Sunderland, MA: Sinauer Associates, Inc.; 2004. 545 p.

109. Good JM, Dean MD, Nachman MW. A complex genetic basis to X-linked hybrid male sterility between two species of house mice. Genetics. 2008;179:2213-28.

110. Crespi BJ, Nosil P. Conflictual speciation: species formation via genomic conflict. Trends in Ecology & Evolution. 2013;28:48-57.

111. Larson EL, Kopania EEK, Good JM. Spermatogenesis and the evolution of mammalian sex chromosomes. Trends in Genetics. 2018;34:722-32.

112. Scribner SJ, Wynne-Edwards KE. Disruption of body-temperature and behavior rhythms during reproduction in dwarf hamster (Phodopus). Physiology & Behavior. 1994;55:361-9.

113. Brekke TD, Steele KA, Mulley JF. Inbred or outbred? Genetic diversity in laboratory rodent colonies. G3-Genes Genomes Genetics. 2018;8:679-86.

114. Ishishita S, Tsuboi K, Ohishi N, Tsuchiya K, Matsuda Y. Abnormal pairing of X and Y sex chromosomes during meiosis I in interspecific hybrids of Phodopus campbelli and P. sungorus. Scientific Reports. 2015;5:9435-9.

115. Peterson BK, Weber JN, Kay EH, Fisher HS, Hoekstra HE. Double Digest RADseq: An Inexpensive Method for De Novo SNP Discovery and Genotyping in Model and Non-Model Species. PloS ONE. 2012;7.

116. Catchen J, Hohenlohe PA, Bassham S, Amores A, Cresko WA. Stacks: an analysis tool set for population genomics. Molecular Ecology. 2013;22:3124-40.

117. Li H, Durbin R. Fast and accurate short read alignment with Burrows-Wheeler transform. Bioinformatics. 2009;25:1754-60.

118. DePristo MA, Banks E, Poplin R, Garimella KV, Maguire JR, Hartl C, et al. A framework for variation discovery and genotyping using next-generation DNA sequencing data. Nature Genetics. 2011;43:491-8.

119. Van der Auwera GA, Carneiro MO, Hartl C, Poplin R, del Angel G, Levy-Moonshine A, et al. From FastQ data to high confidence variant calls: the Genome Analysis Toolkit best practices pipeline. Current protocols in bioinformatics / editoral board, Andreas D Baxevanis [et al]. 2013;43:11-33.

120. Kent WJ. BLAT - The BLAST-like alignment tool. Genome Research. 2002;12:656-64.

121. Meyer M, Kircher M. Illumina sequencing library preparation for highly multiplexed target capture and sequencing. Cold Spring Harbor Protocols. 2010;2010:pdb.prot5448.

122. Martin M. Cutadapt removes adapter sequences from high-throughput sequencing reads. EMBnetjournal. 2011;17:1–3.

123. Bolger AM, Lohse M, Usadel B. Trimmomatic: a flexible trimmer for Illumina sequence data. Bioinformatics. 2014;30:2114-20.

124. Broman KW, Sen S. A guide to QTL mapping with R/qtl. New York: Springer; 2009.

125. Haley CS, Knott SA. A simple regression method for mapping quantitative trait loci in line crosses using flanking markers. Heredity. 1992;69:315-24.

126. Feenstra B, Skovgaard IM, Broman KW. Mapping quantitative trait loci by an extension of the Haley-Knott regression method using estimating equations. Genetics. 2006;173:2269-82.

127. Brekke TD, Supriya S, Denver MG, Thom A, Steele KA, Mulley JF. A high-density genetic map and molecular sex-typing assay for gerbils. Mammalian Genome. 2019;30:63-70.

128. Wang Z, Gerstein M, Snyder M. RNA-Seq: a revolutionary tool for transcriptomics. Nature Reviews Genetics. 2009;10:57-63.

129. Langmead B, Salzberg SL. Fast gapped-read alignment with Bowtie 2. Nature Methods. 2012;9:357-9.

130. Liao Y, Smyth GK, Shi W. featureCounts: an efficient general purpose program for assigning sequence reads to genomic features. Bioinformatics. 2014;30:923-30.

131. Robinson MD, Oshlack A. A scaling normalization method for differential expression analysis of RNA-seq data. Genome Biology. 2010;11:R25.

132. Langfelder P, Horvath S. WGCNA: an R package for weighted correlation network analysis. BMC Bioinformatics. 2008;9.

133. Storey JD, Bass AJ, Dabney A, Robinson D. qvalue: Q-value estimation for false discovery rate control. R package version 2.18.0. ed2019.

134. Huang S, Kao C-Y, McMillan L, Wang W. Transforming genomes using MOD files with applications. Proceedings of the ACM Conference on Bioinformatics, Computational Biology and Biomedicine. 2013;10.1145/2506583.2506643:595-604.

135. Huang S, Holt J, Kao C-Y, McMillan L, Wang W. A novel multi-alignment pipeline for high-throughput sequencing data. Database. 2014;2014:bau057.

136. Ouellette LA, Reid RW, Blanchard SG, Brouwer CR. LinkageMapView-rendering high-resolution linkage and QTL maps. Bioinformatics. 2018;34:306-7.

137. Manshouri R, Coyaud E, Kundu ST, Peng DH, Stratton SA, Alton K, et al. ZEB1/NuRD complex suppresses TBC1D2b to stimulate E-cadherin internalization and promote metastasis in lung cancer. Nature Communications. 2019;10:5125.

138. Miljkovic-Licina M, Hammel P, Garrido-Urbani S, Lee BPL, Meguenani M, Chaabane C, et al. Targeting Olfactomedin-like 3 inhibits tumor growth by impairing angiogenesis and pericyte coverage. Molecular Cancer Therapeutics. 2012;11:2588-99.

139. Karabag T, Kaya A, Temizhan A, Koc F, Yavuz S, Cam S. The influence of homocysteine levels on endothelial function and their relation with microvascular complications in T2DM patients without macrovascular disease. Acta Diabetologica. 2007;44:69-75.

140. Muszbek L, Bereczky Z, Bagoly Z, Komaromi I, Katona E. Factor XIII: a coagulation factor with multiple plasmatic and cellular functions Physiological Reviews. 2011;91:931-72.

141. Stefanovic B, Manojlovic Z, Vied C, Badger CD, Stefanovic L. Discovery and evaluation of inhibitor of LARP6 as specific antifibrotic compound. Scientific Reports. 2019;9:326.

142. Wilder JA, Hewett EK, Gansner ME. Molecular Evolution of GYPC: Evidence for Recent Structural Innovation and Positive Selection in Humans. Molecular Biology and Evolution. 2009;26:2679-87.

Supplemental Information

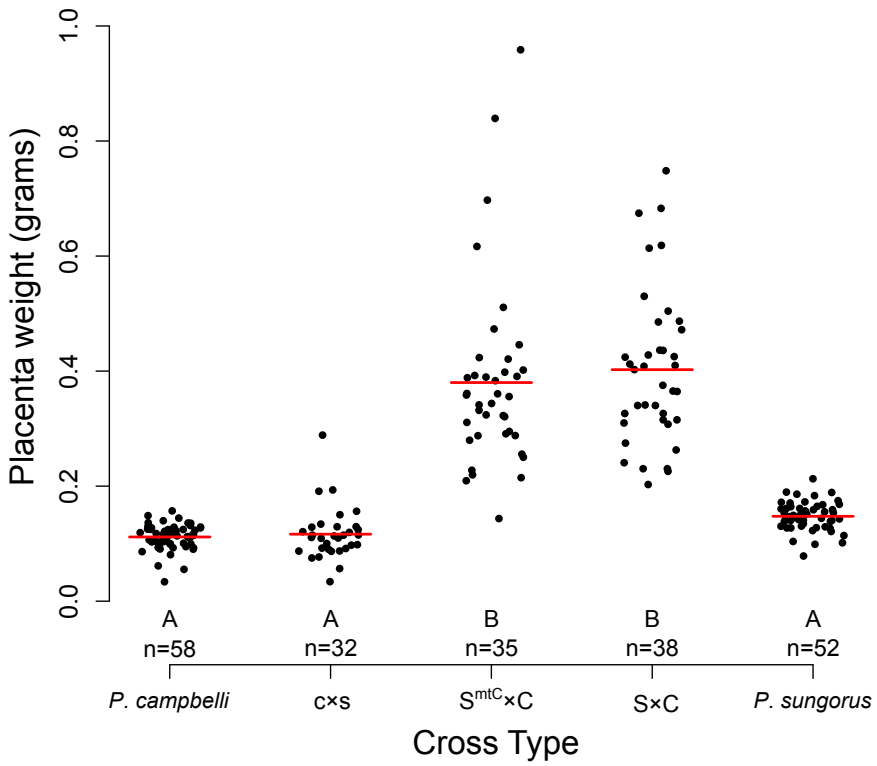

Figure S1. Mitochondria have no effect on placenta size. If an interaction involving the *P. sungorus* mitochondria causes overgrowth, the placentas from the S^{mtC}×C cross should be similar to the parental type. Instead they are indistinguishable from S×C hybrids ($F_{4,213}$ = 106, P<0.001, ANOVA). Data for *P. campbelli*, c×s, S×C, and *P. sungorus* from [33]. Statistically significant groups 'A' and 'B' were assigned with a Tukey HSD test.

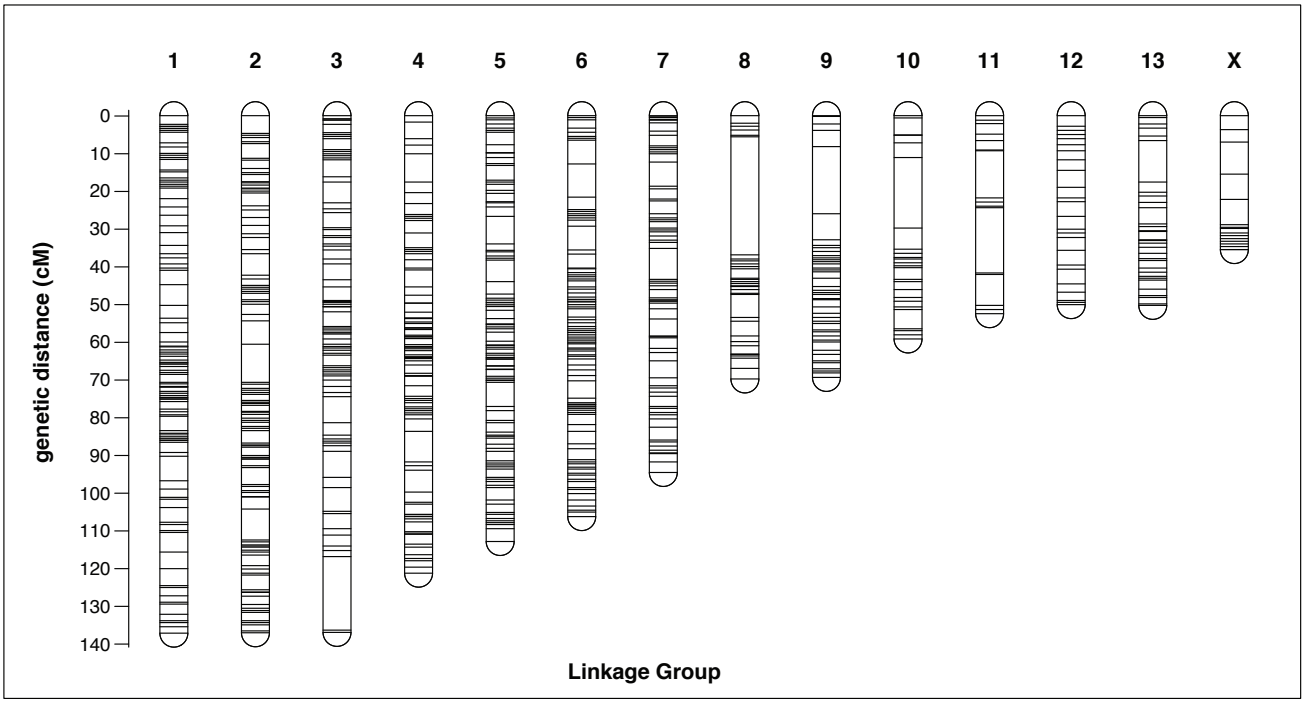

Figure S2. Genetic map of *Phodopus* dwarf hamsters. This map includes 1,215 RAD markers and spans 1,213.7cM across 13 autosomal linkage groups and the X chromosome. Linkage groups are numbered by decreasing length. The sequence of each marker and their exact locations in centiMorgans can be found in Supplemental Table 1. Specific locations of genes can be found in Supplemental Table 2. visualized with r/LinkageMapView [136].

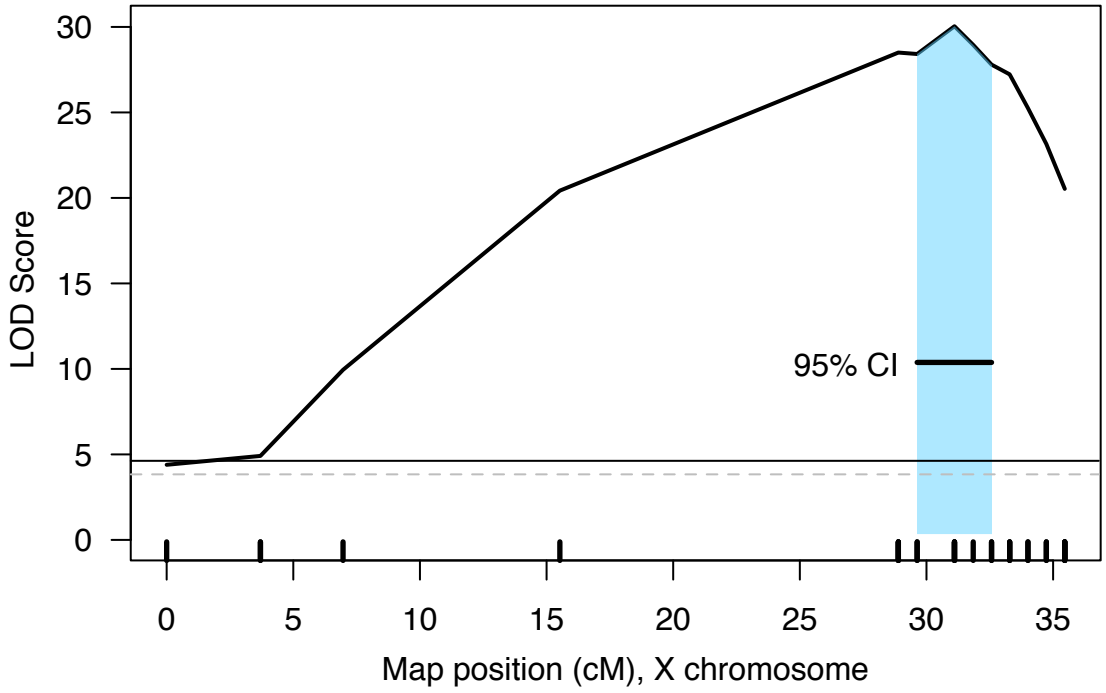

Figure S3. QTL interval on the X chromosome overlaps with increased marker density. Placental weight QTL likely corresponds to region of reduced recombination on the map. Solid line indicates permutation-based P = 0.01 significance threshold, dashed line indicates permutation-based P = 0.05 significance threshold.

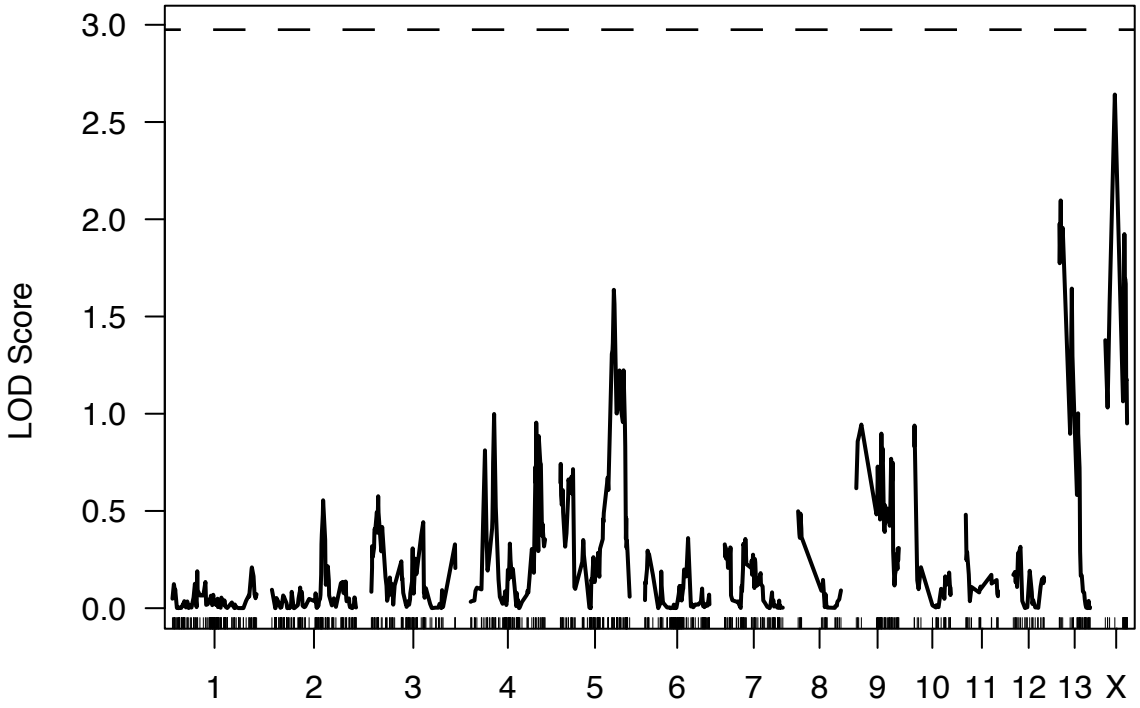

Figure S4. No QTL for embryo weight detectable in the BC mapping experiment. No peak passes the permutation threshold when controlling for Theiler stage and edema, P = 0.05 permutation threshold indicated with dashed line.

Supplemental Information

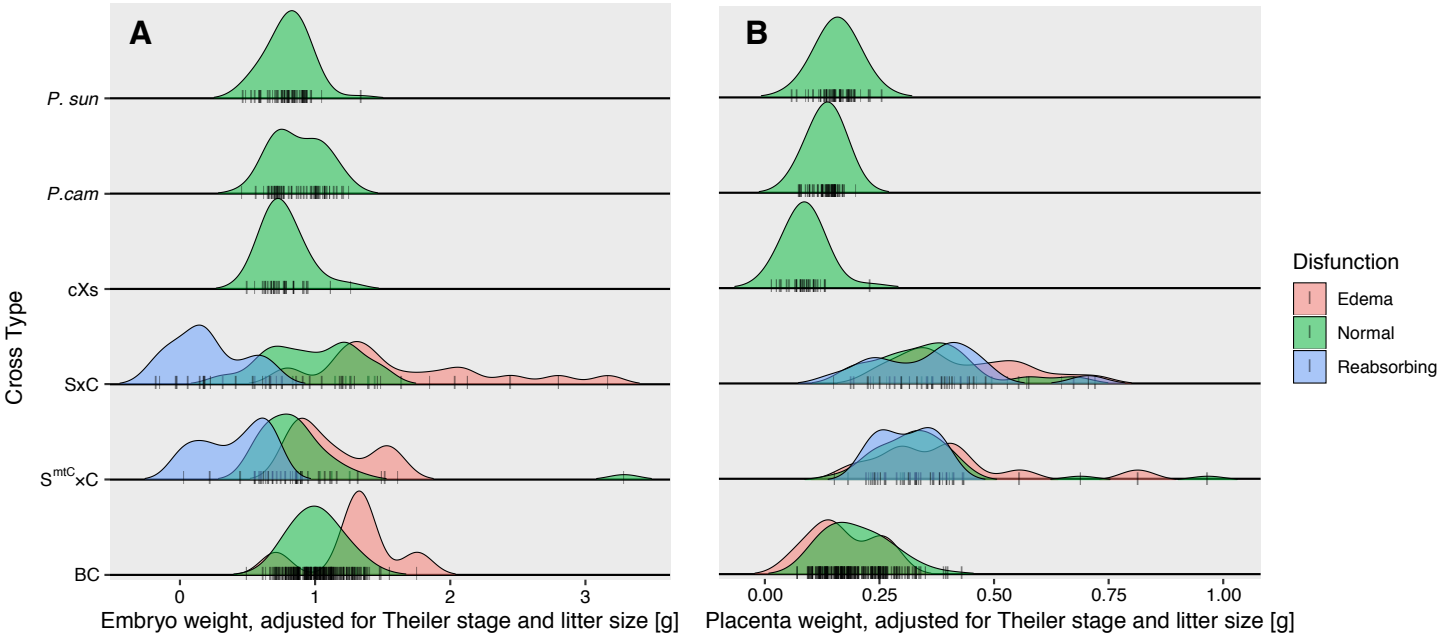

Figure S5. Edema and reabsorption explain much of the variance in embryo size, but not placenta size, in interspecies hybrid hamsters. Reabsorption (blue) and edema (red) shift embryo size away from the mean in *P. sungorus* x *P. campbelli* (SxC) F_1, SxC mitochondrial introgression, and BC hybrid hamsters (A), but have little effect on placenta size (B).

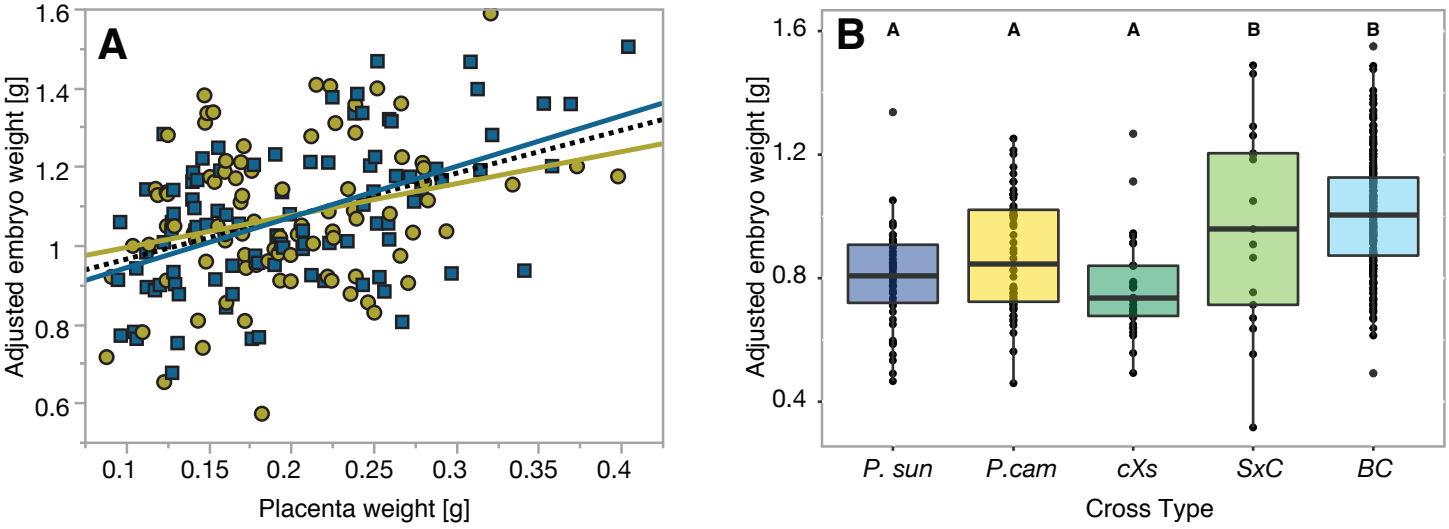

Figure S6. Embryo weight in the BC. Embryo weight is positively associated with placental weight in the BC, more strongly in males (blue, adjusted r2 = 0.257, $F_{1,95}$ = 33.8, P << 0.0001) than females (yellow, adjusted r2 = 0.065, $F_{1,88}$ = 7.15, P = 0.0090). When BC embryo weights are analyzed along with F_1 hybrids, the overgrown SxC F_1 and BC hybrids show a slight but significant increase in size controlling for stage and edema (adjusted r2 = 0.159, $F_{1,184}$ = 36.0, P << 0.0001, ANOVA)

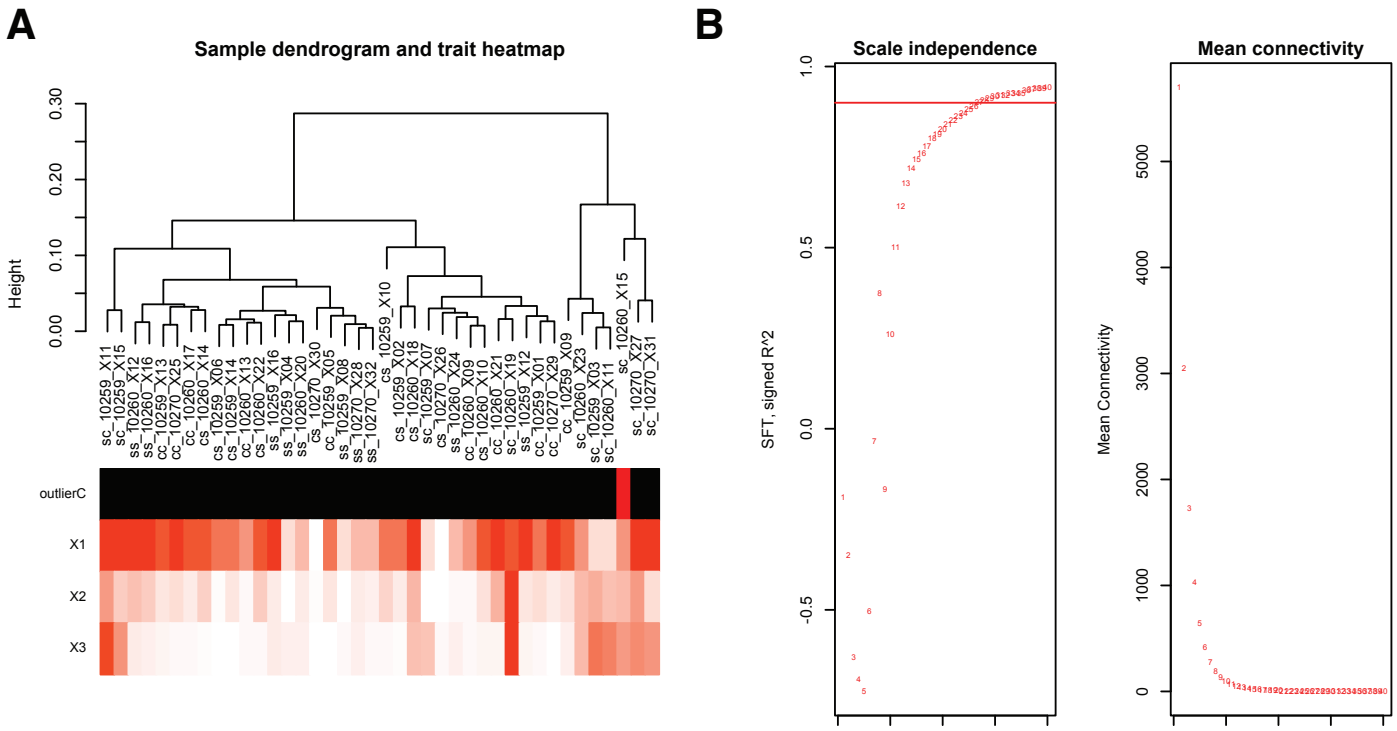

Figure S7. Standard WGCNA output, F_1 data. (A) Outlier identification of sample to be removed in red. (B) Dynamic thresholding.

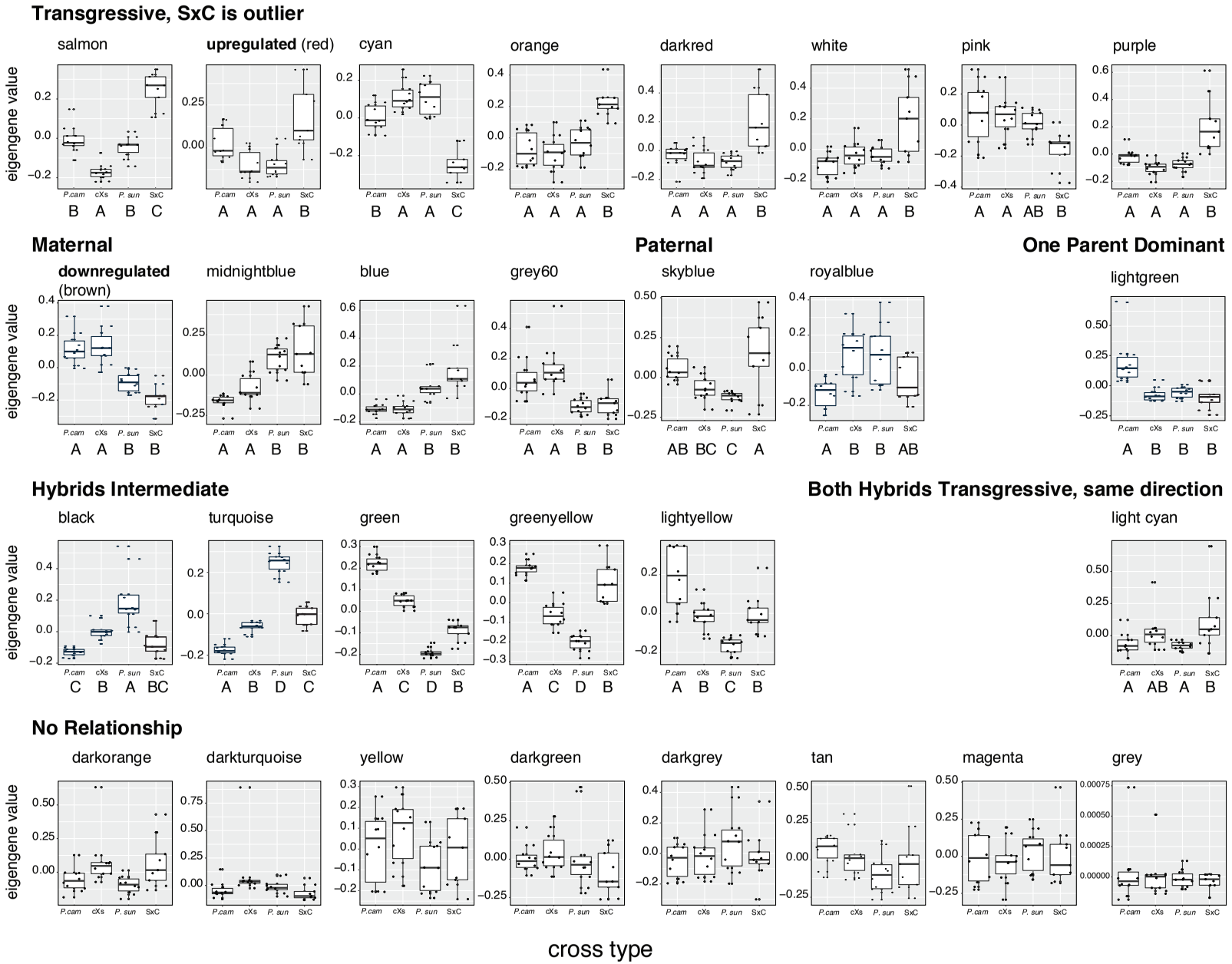

Figure S8. Assignment of inheritance patterns of modules in network. Summary values of module expression (module eigengene) tested with an ANOVA to identify parent of origin and transgressive expression. Color names are arbitrarily and randomly generated by the program, and have no additional meaning. Letters indicate Tukey HSD assigned significance groups at $p<0.05$.

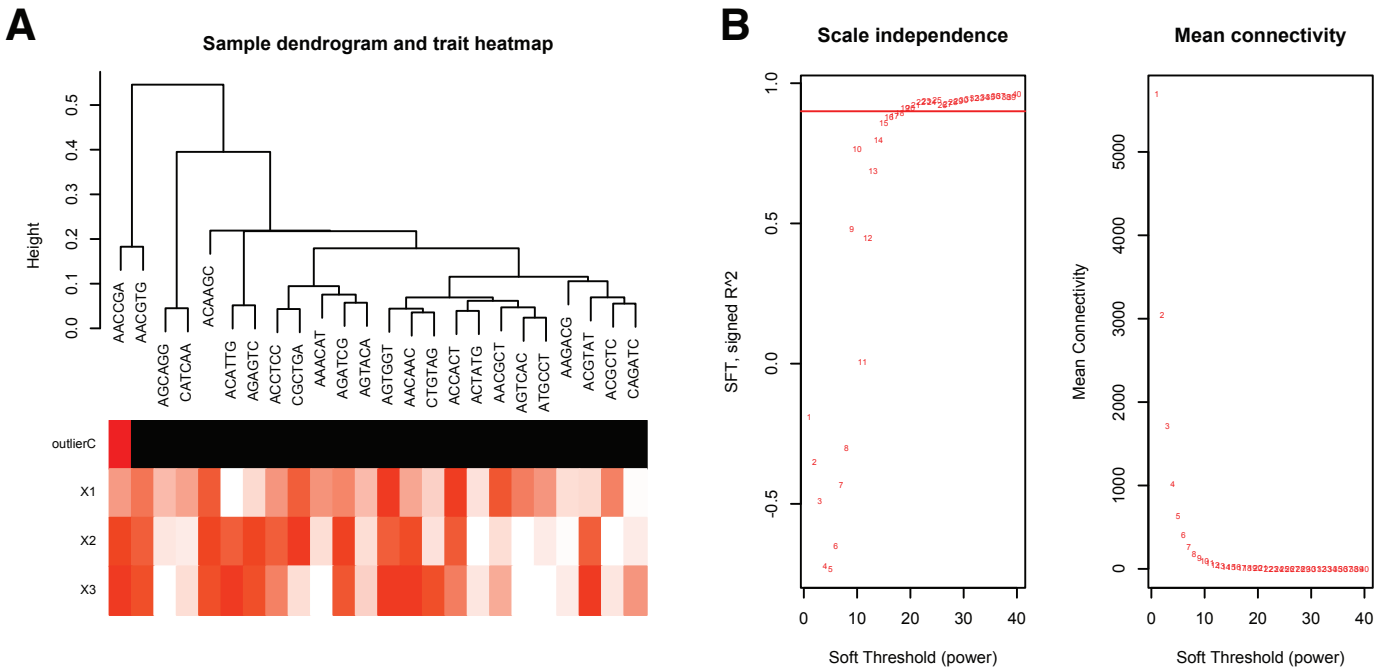

Figure S9. Standard WGCNA output, BC data. (A) Outlier identification of sample to be removed in red. (B) Dynamic thresholding.

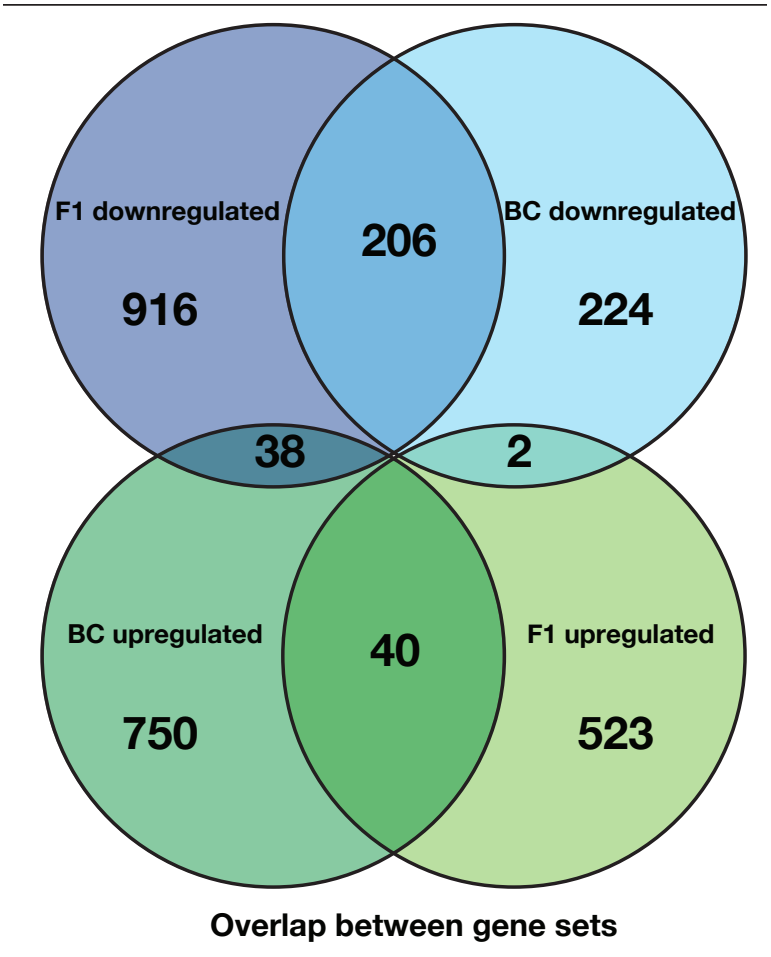

Figure S10. Count overlap between key F_1 and BC modules. Venn diagram showing counts of genes shared between F_1 and BC downregulated and upregulated placenta modules. The downregulated modules share the most genes (206).

Supplemental Information

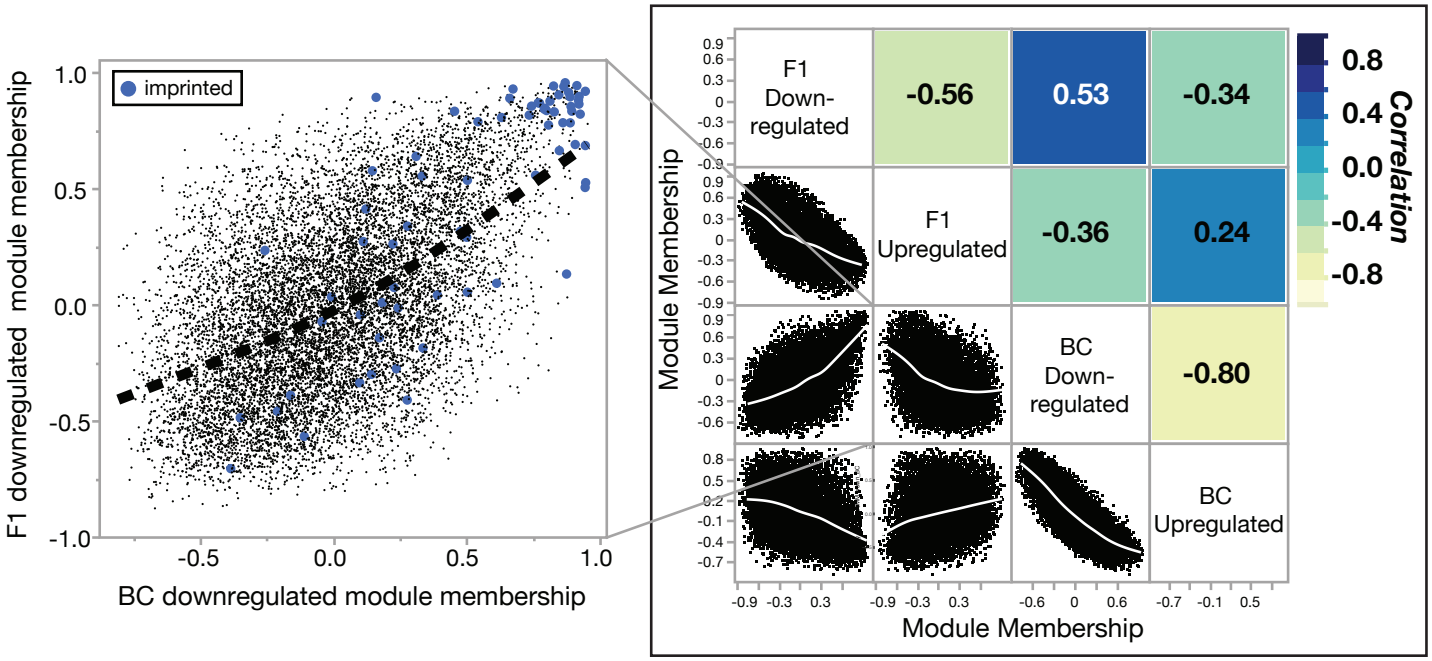

Figure S11. Correlation between key F_1 and BC modules. Each gene in the network has a correlation to each module eigengene, whether that gene is placed in the module or not. We can assess how similar two modules are by asking whether genes are generally showing the same bivariate correlation to each module. Not only are the downregulated and upregulated modules within each data set negatively correlated with each other (F_1, Pearson's R = -0.56, p<0.0001, BC, Pearson's R = -0.80, p<0.0001), the F_1 and BC downregulated modules across experiments are positively correlated with each other (Pearson's R = 0.53, p<0.0001). Notably, the same candidate imprinted genes share high connectivity/module membership with the network in both data sets (blue dots, inset).

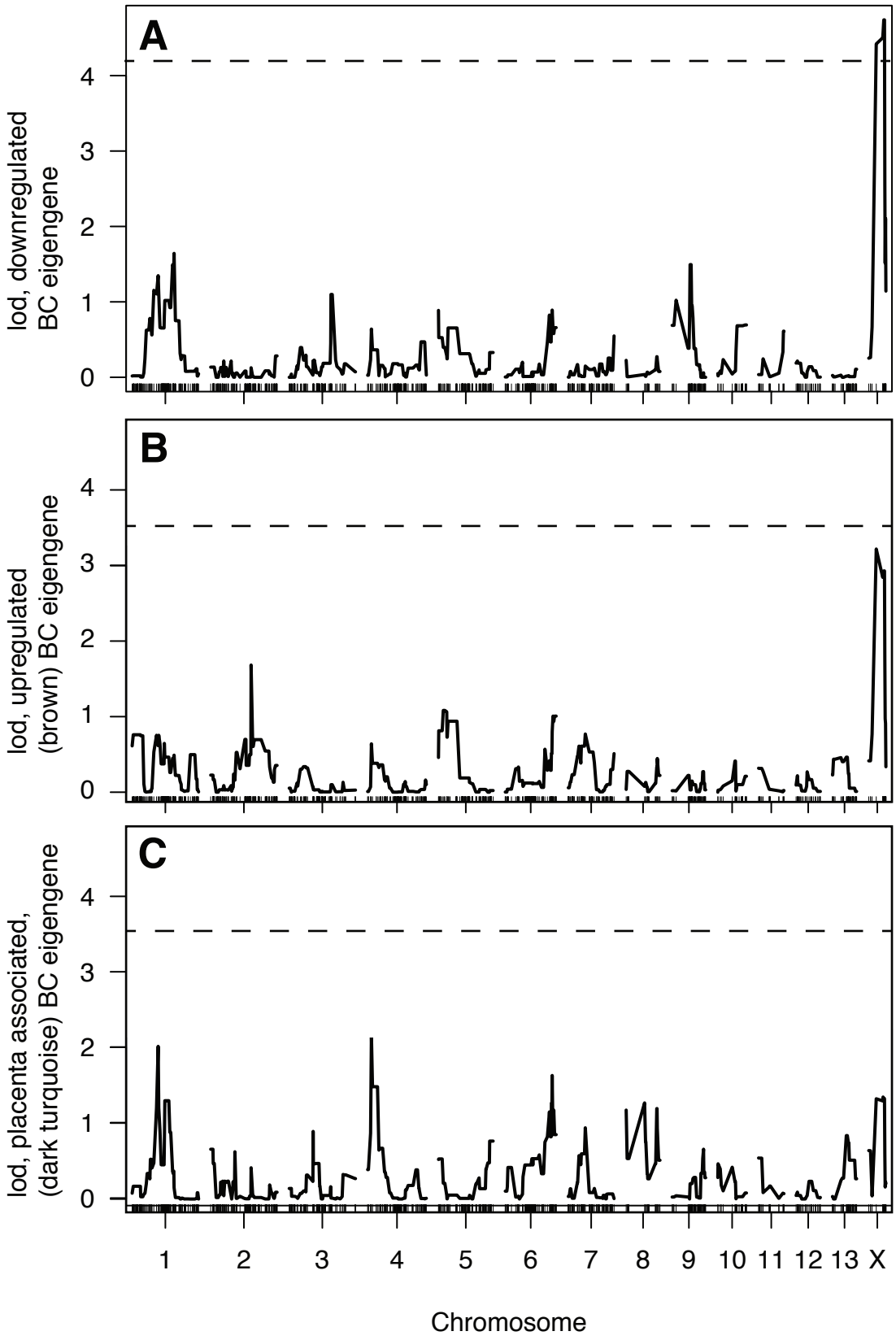

Figure S12. eigenQTL in BC hybrids. Using the module summary eigengene as a phenotype to explain the genetic basis of gene expression patterns in 23 BC hybrids, we find that the downregulated module has a single QTL on the X that passes a p=0.05 permutation threshold (QTL peak at 31.1cM, LOD=4.739) (A), but that the others tested do not (B,C). Dashed line indicates permutation-based P = 0.05 significance threshold.

Supplemental Information

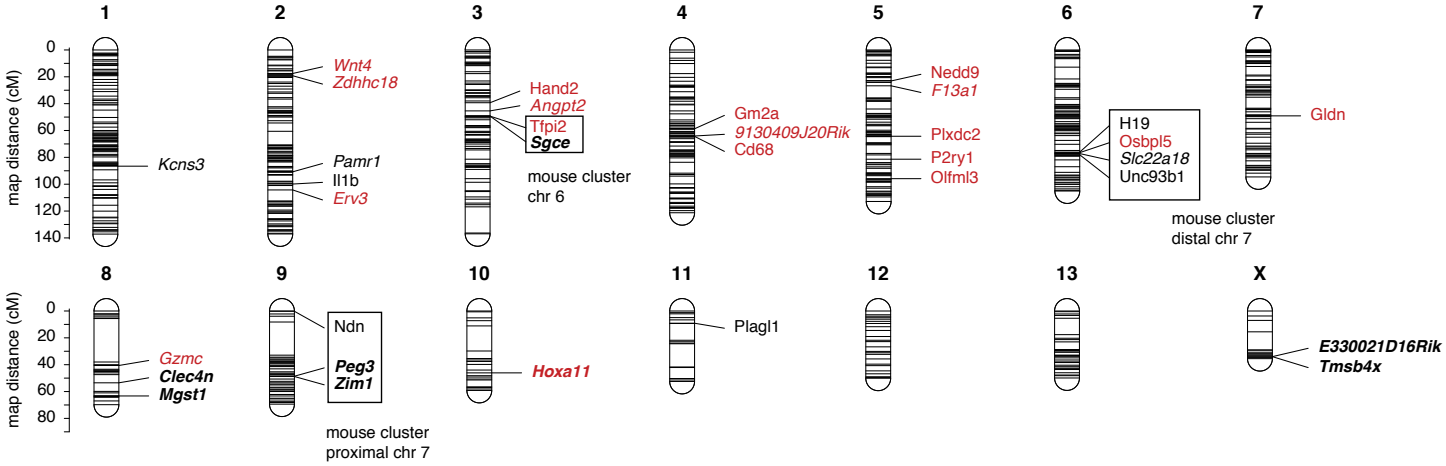

Figure S13. Candidate imprinted genes placed on the genetic map. Candidate imprinted genes that are in the BC downregulated network are indicated in red, and clusters with probable homology to imprinted clusters in *Mus* are indicated with boxes. Visualized with r/LinkageMapView [136].

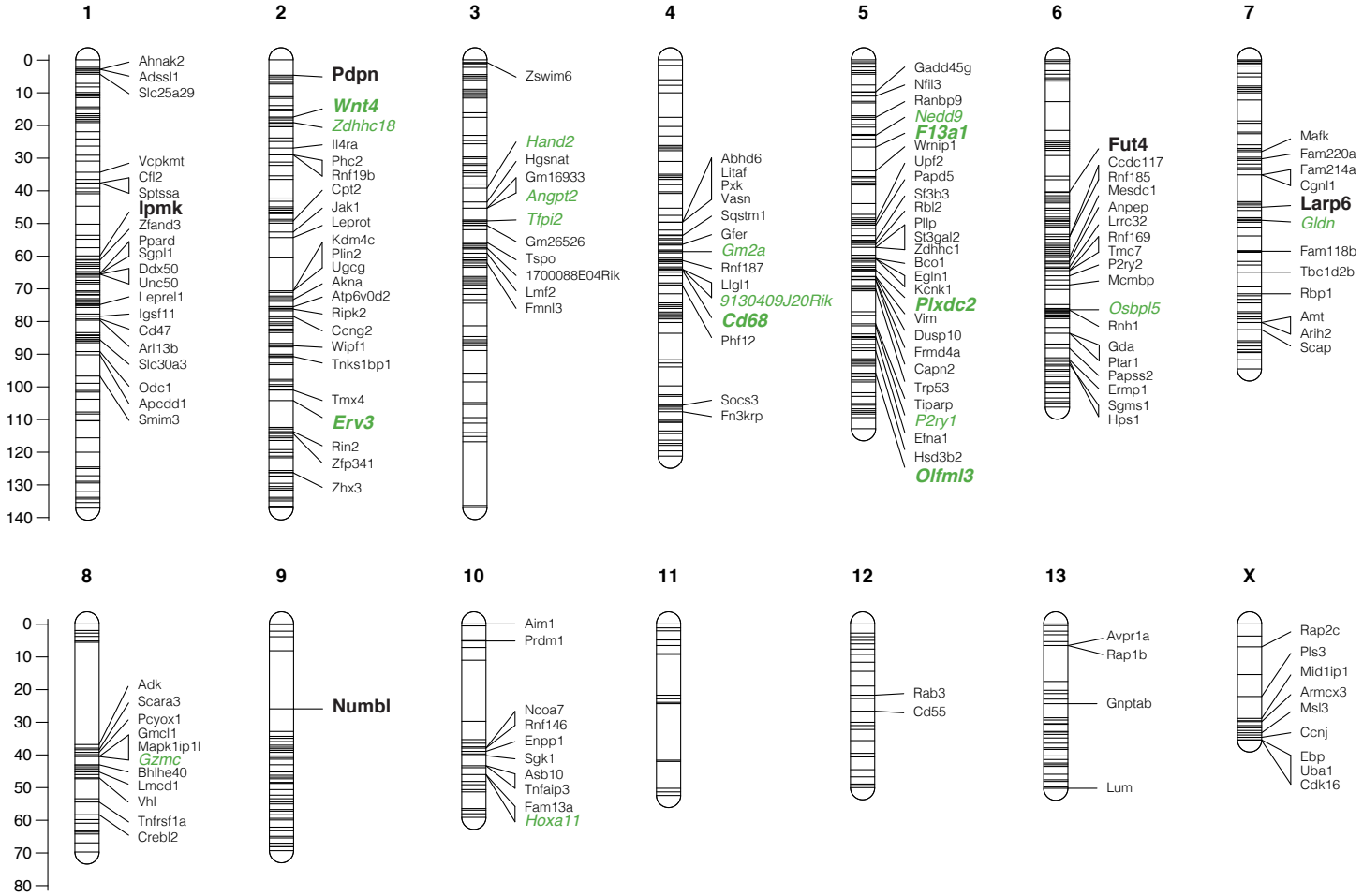

Figure S14. BC downregulated module placed on the genetic map. BC downregulated network hub genes are in bold, and candidate imprinted are indicated in green. Visualized with r/LinkageMapView [136].

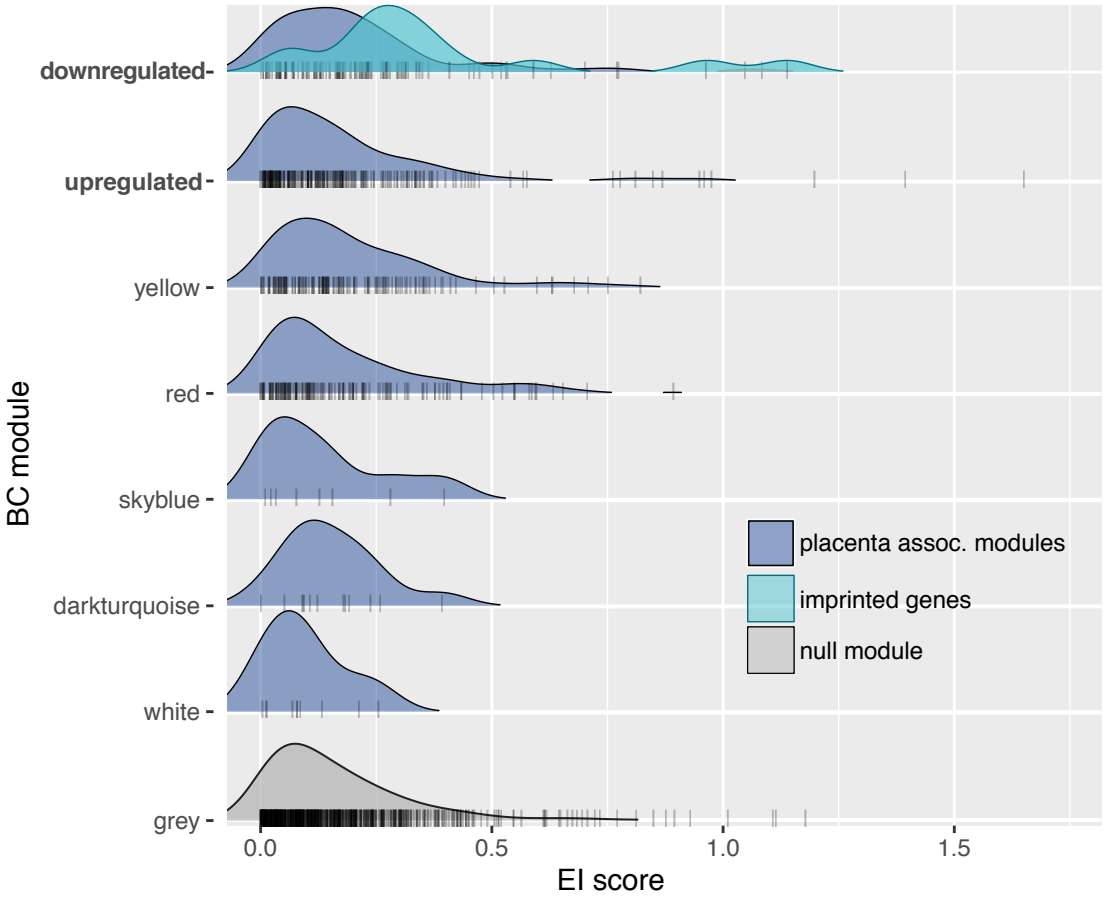

Figure S15. EI score distributions by module and imprinting status. The grey module includes all genes that were not placed in any module in the network analysis, and serves as the null expectation of the distribution of the score. All BC modules associated with placenta size are included here, with shift of increased EI values for the candidate imprinted genes in the downregulated module, but not the other placenta associated modules.

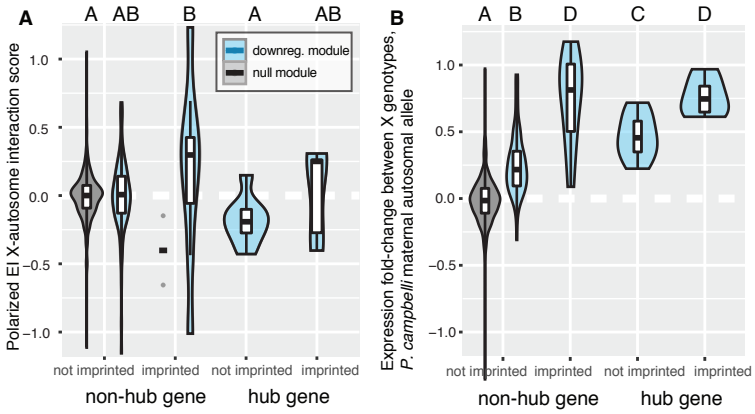

Figure S16. Polarized EI score distributions by hub and imprinting status. Polarized expression interaction scores (A) show that imprinted genes are more likely to have a larger fold change when the maternal alleles are mismatched with the maternal X chromosome (a positive value). (B) Positive values for gene expression fold change between X genotypes for individuals with a (mismatched) homozygous *P. campbelli* autosomal genotype indicate that expression is higher for individuals with a *P. campbelli* X chromosome than for those with a *P. sungorus* X chromosome. All letter groups indicate Tukey HSD significance at $P < 0.05$.

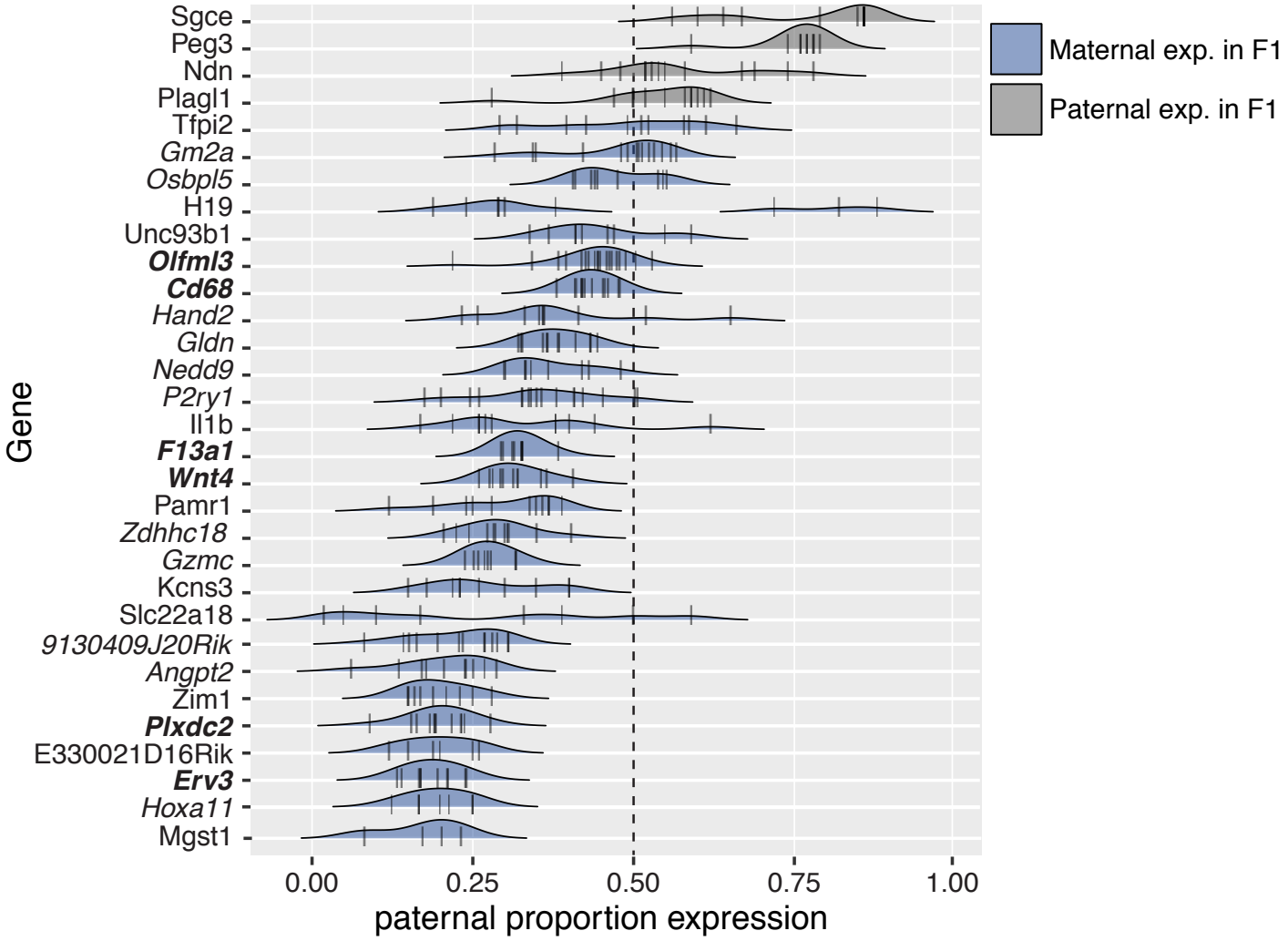

Figure S17. Allelic bias in candidate imprinted genes in BC. Proportion of paternal expression for all heterozygous BC hybrids for each of the 31 candidate imprinted genes that were placed on the map. Generally, we recover the signal for maternal bias in genes that displayed maternal bias in the F_1s (blue), and paternal bias for those genes with paternal bias in the F_1s (grey). Bolded genes are hub genes in the BC downregulated module.

Table S1. A full description of all RAD markers including their ID, the linkage group they are found on, the position in centiMorgans on that linkage group, the base position of the SNV between *P. campbelli* and *P. sungorus*, the alleles for *P. campbelli* and *P. sungorus*, and the sequence of the marker which always begin with TGCAGG (the restriction-enzyme cut-site of SbfI, i.e.: CC_TGCA^GG). SNVs in the sequence are denoted with standard IUPAC ambiguity codes.

Table S2. WGCNA modules generated from F_1 and pure species placental gene expression data. Color names are arbitrarily and randomly generated by the program, and have no additional meaning. The upregulated and downregulated modules are discussed in the manuscript are indicated as such. Counts of genes in each module, correspondence with previous pairwise analysis [38], association with inheritance pattern and phenotypes, and enrichment for candidate imprinted genes indicated.

Table S3. WGCNA modules generated from BC placental gene expression data. As before, color names are arbitrarily and randomly generated by the program, and do not correspond whatsoever with the arbitrarily assigned names given to the F_1 data. The upregulated and downregulated modules are discussed in the manuscript are indicated as such. Counts of genes in each module, correspondence with F_1 network analysis, association with phenotypes, and enrichment for candidate imprinted genes indicated.

Table S4. A full description of the locations of each gene from that was captured and associated with the map. Columns are: Linkage group, position in centiMorgans, gene name from the *P. sungorus* transcriptome (Genbank BioProject JNA306772, DDBJ/EMBL/GenBank Accession GEVB00000000, [38]), the exon that the SNP appears in, the position of the SNP in the exon, the gene name, and the mouse ensemble gene ID of that gene.

Table S5. SRA sequence accession numbers for each individual by sequence type.